Supplement of Biogeosciences Discuss., 11, 15693–15732, 2014
http://www.biogeosciences-discuss.net/11/15693/2014/
doi:10.5194/bgd-11-15693-2014-supplement

Biogeosciences
Discussions
Open Access

Supplement of

Marine sources of bromoform in the global open ocean – global patterns and emissions

I. Stemmler et al.

Correspondence to: I. Stemmler (irene.stemmler@uni-hamburg.de)

1 Simulated bromoform concentrations

1.1 MPIOM-HAMOCC simulations

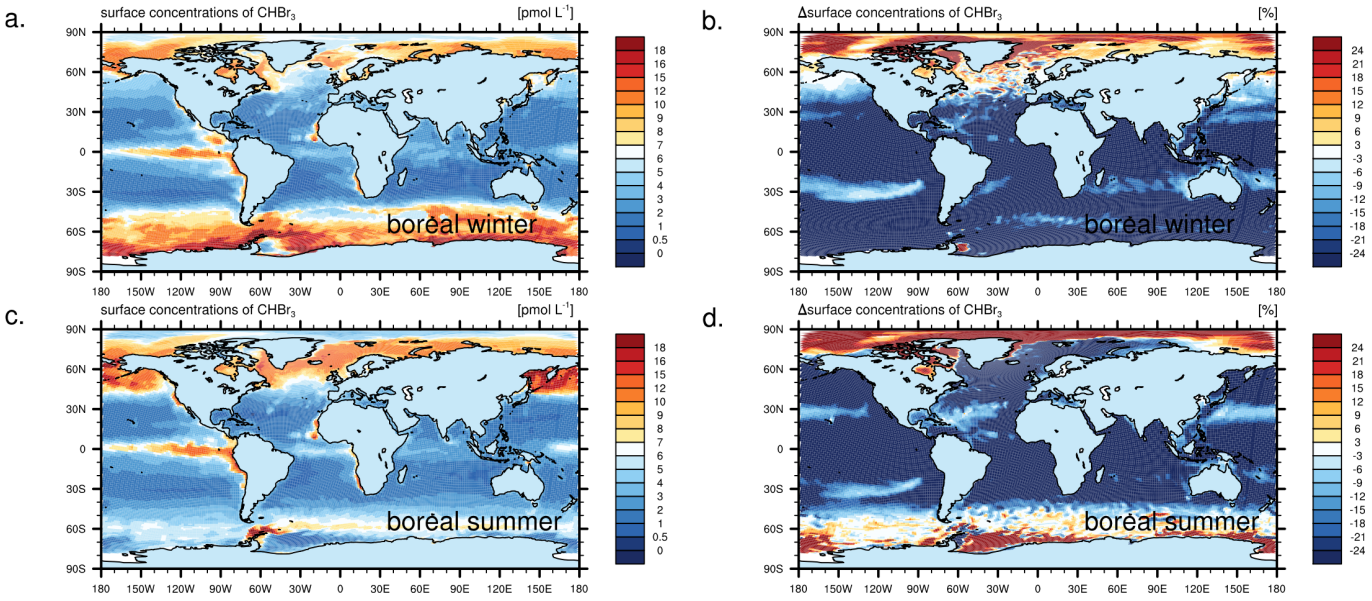

Figure S1 Bromform surface concentrations [pmol L^{-1}] in boreal winter and summer in experiment Clim-at (a, c) and percentage differences to concentrations in experiment Equi ($100 \cdot \frac{\text{Equi}-\text{Clim}-\text{at}}{\text{Clim}-\text{at}}$) (b, d).

2 Simulated and observed bromoform concentrations and net primary productivity

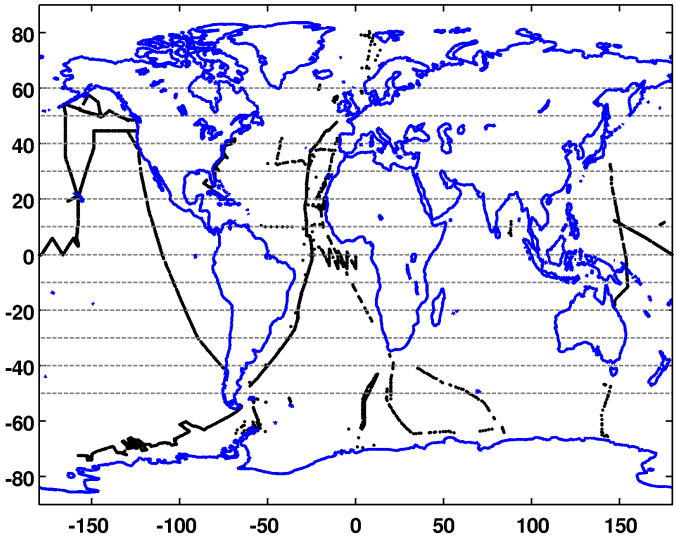

Figure S2 Locations of bromoform observations. Dashed gray lines show margins of latitudinal boxes used in the Box-Whisker plots.

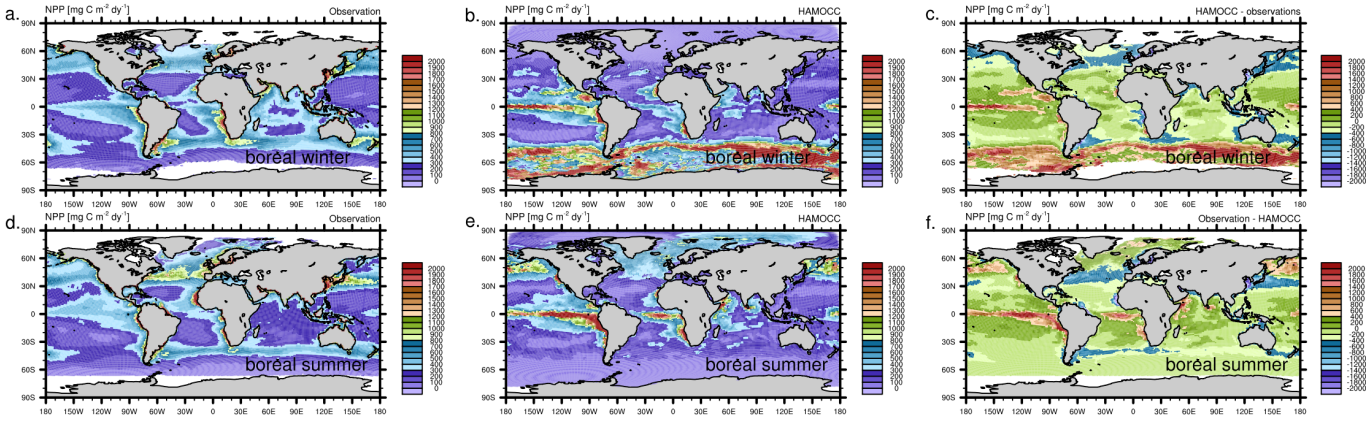

Figure S3 Simulated (b, e) and observation-based (a, d) net primary productivity [mg C m^{-2} dy^{-1}] and their difference (c, f). The observation-based NPP product is based on data 1997-2009 from SeaWiFS Chl-*a*, PAR and AVHRR SST and derived using the VGPM model (Behrenfeld and Falkowski, 1997). The NPP producted was downloaded from http://wiki.icess.ucsb.edu/measures/NPP_Products (accessed June 2014).

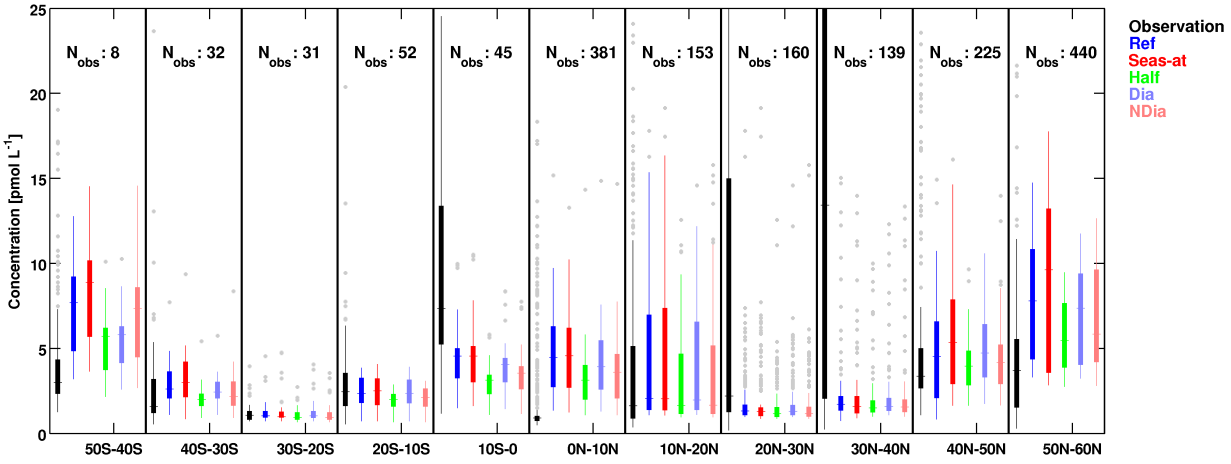

Figure S4 Box-Whisker plot of simulated and observed surface ocean bromoform concentrations pmol L^{-1} in the Pacific. Box widths are determined by the 25% and 75% percentile of data within each 10 degree latitude box, outliers (gray) are located outside 1.5 times the differences of the percentiles, the middle line of each box shows the median. Simulated concentrations are averaged over 1 degree boxes around the location of observations. Different colors denote different experiments; observations are shown in black.

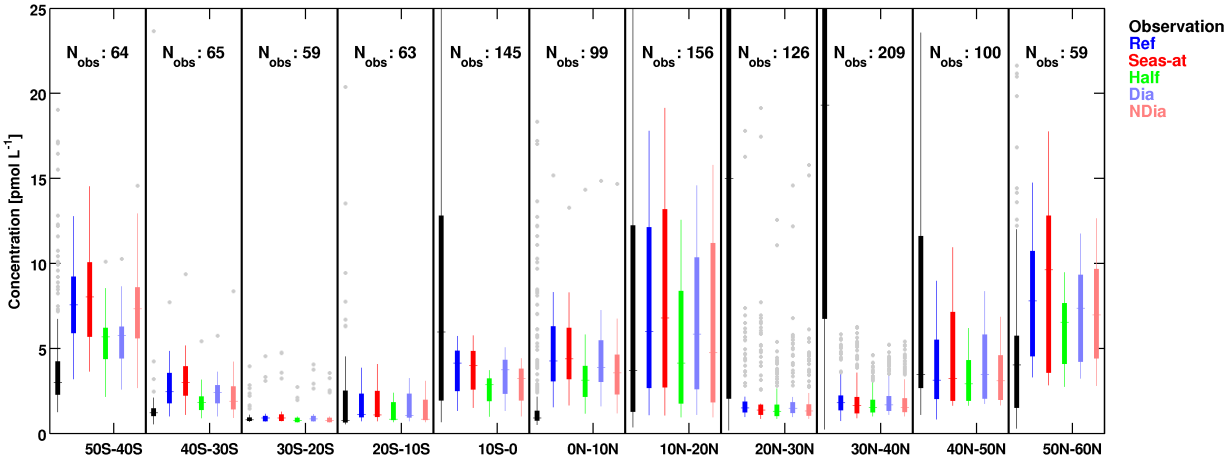

Figure S5 Box-Whisker plot of simulated and observed surface ocean bromoform concentrations pmol L^{-1} in the Atlantic. Box widths are determined by the 25% and 75% percentile of data within each 10 degree latitude box, outliers (gray) are located outside 1.5 times the differences of the percentiles, the middle line of each box shows the median. Simulated concentrations are averaged over 1 degree boxes around the location of observations. Different colors denote different experiments; observations are shown in black.

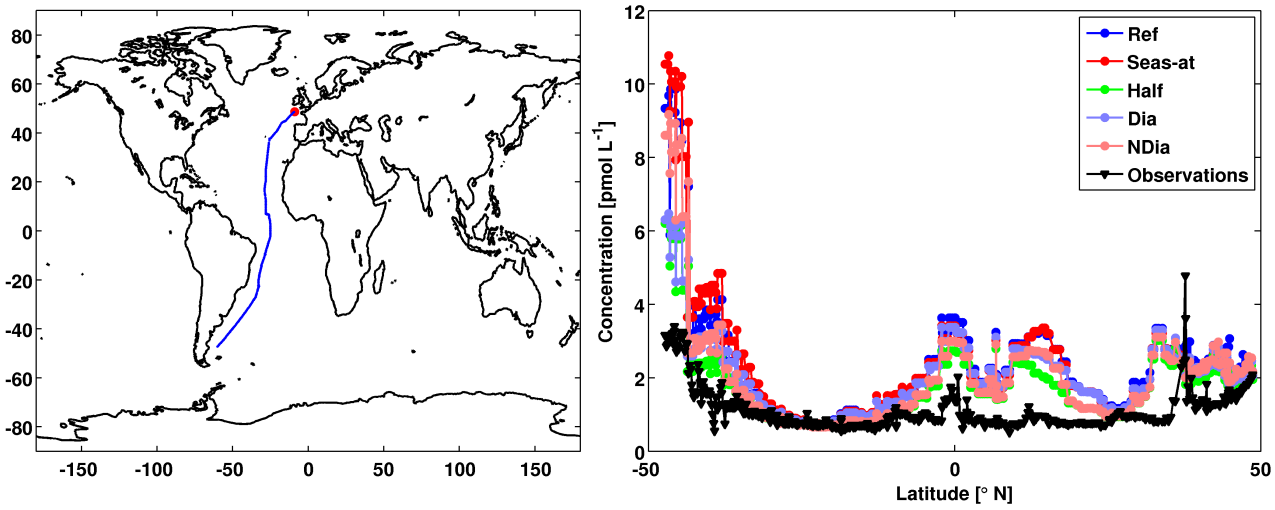

Figure S6 Simulated and observed bromoform concentrations [pmol L^{-1}]. Observations are from the Polarstern cruise BLAST 2, 18.10.-21.11.1994 (Butler et al., 2007) as listed in the SI of (Ziska et al., 2013).

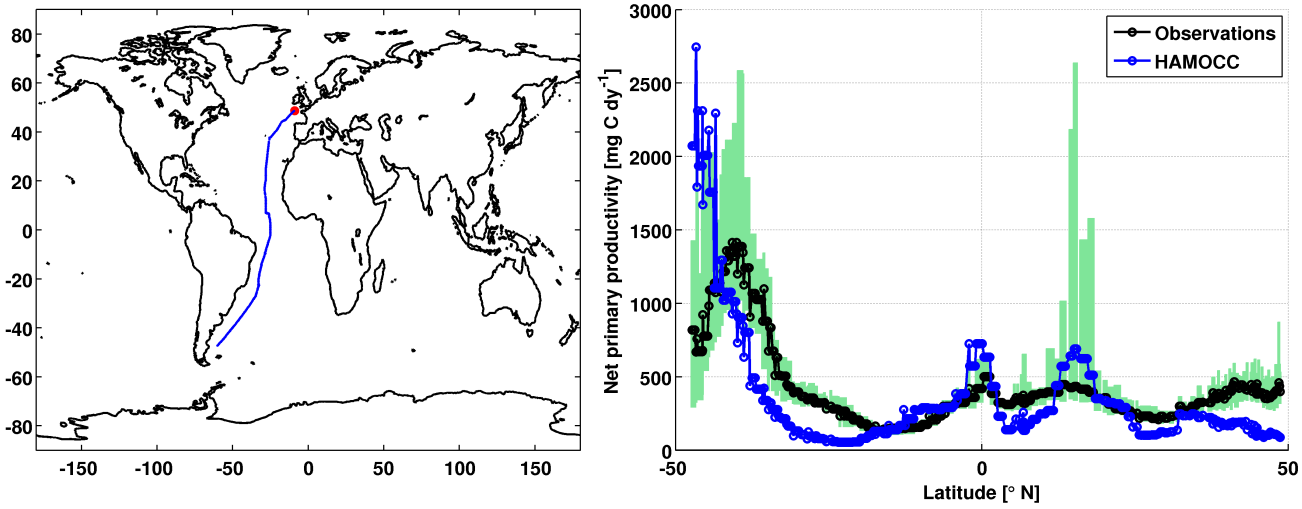

Figure S7 Simulated and observation-based net primary productivity [mg C m^{-2} dy^{-1}]. Green shades show mimimum and maximum range of the observation-based estimate, the black dashed line shows the median. The observation-based NPP product is based on data 1997-2009 from SeaWiFS Chl-*a*, PAR and AVHRR SST and derived using the VGPM model (Behrenfeld and Falkowski, 1997). The NPP producted was downloaded from http://wiki.icess.ucsb.edu/measures/NPP_Products (accessed June 2014).

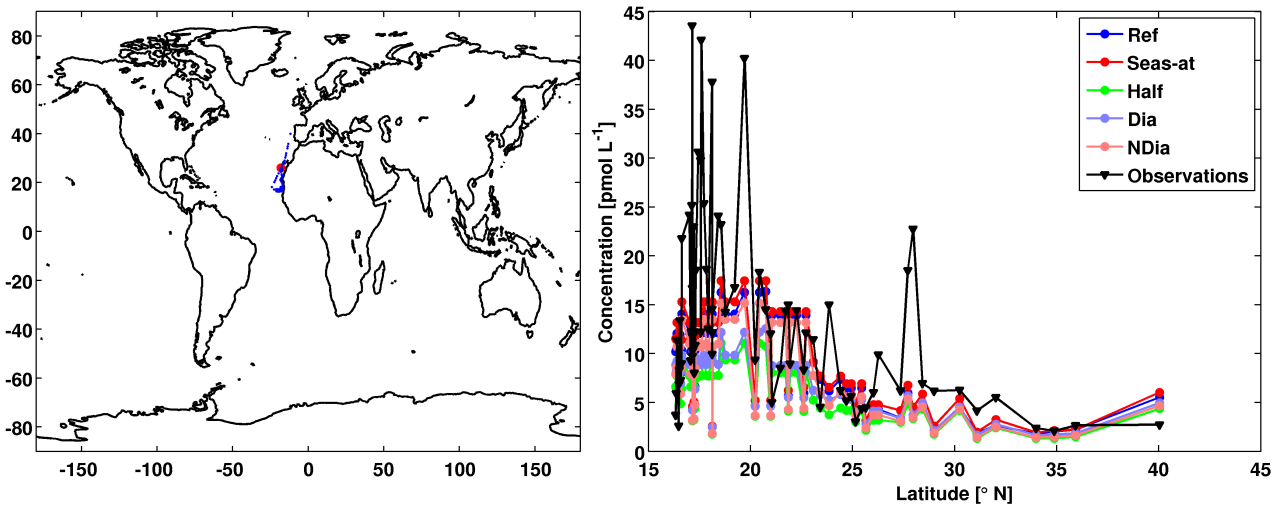

Figure S8 Observations are from a RSS Discovery cruise in May 2007 (EXPOCODE: 74DI20070520) (Jones et al., 2010) as listed in the SI of (Ziska et al., 2013).

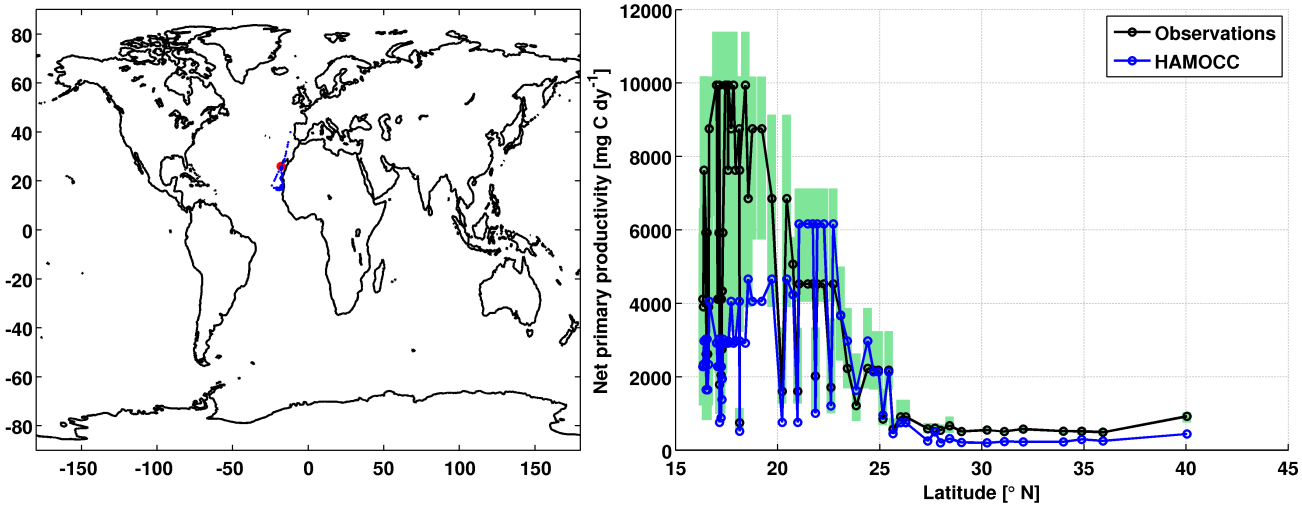

Figure S9 Simulated and observation-based net primary productivity [mg C m^{-2} dy^{-1}]. Green shades show mimimum and maximum range of the observation-based estimate, the black dashed line shows the median. The observation-based NPP product is based on data 1997-2009 from SeaWiFS Chl-*a*, PAR and AVHRR SST and derived using the VGPM model (Behrenfeld and Falkowski, 1997). The NPP producted was downloaded from http://wiki.icess.ucsb.edu/measures/NPP_Products (accessed June 2014).

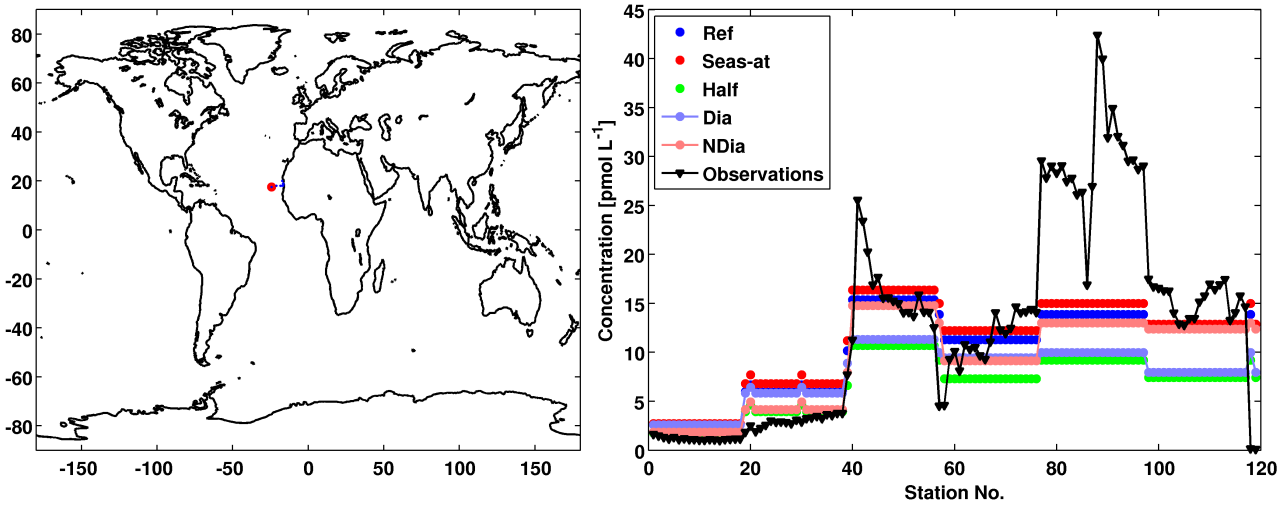

Figure S10 Observations are from the Poseidoin cruise DRIVE in June 2010 as listed in the SI of (Ziska et al., 2013).

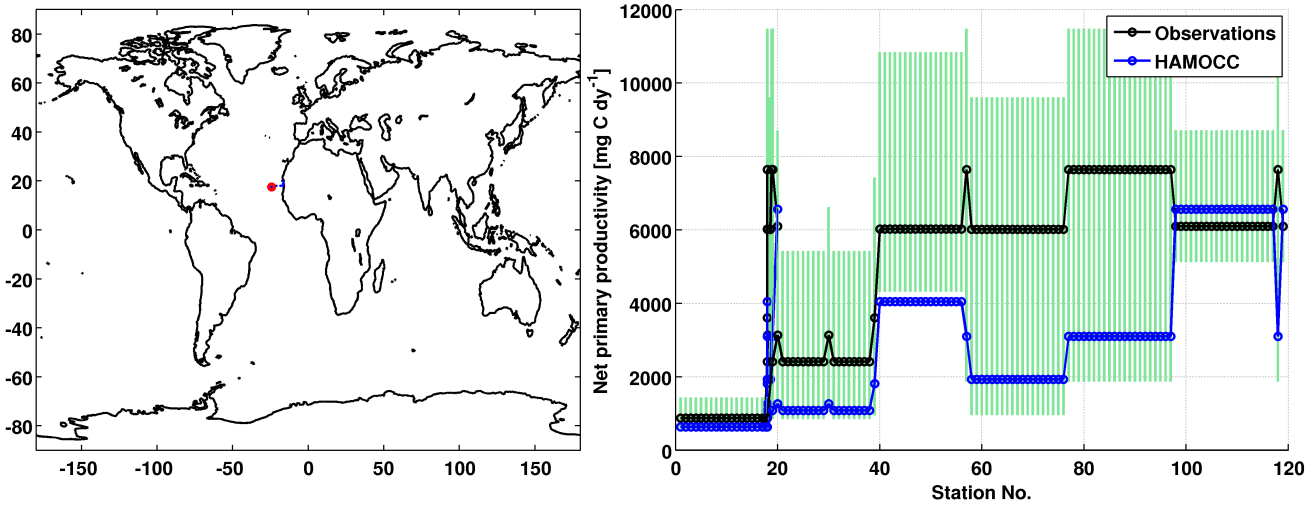

Figure S11 Simulated and observation-based net primary productivity [mg C m^{-2} dy^{-1}]. Green shades show mimimum and maximum range of the observation-based estimate, the black dashed line shows the median. The observation-based NPP product is based on data 1997-2009 from SeaWiFS Chl-*a*, PAR and AVHRR SST and derived using the VGPM model (Behrenfeld and Falkowski, 1997). The NPP producted was downloaded from http://wiki.icess.ucsb.edu/measures/NPP_Products (accessed June 2014).

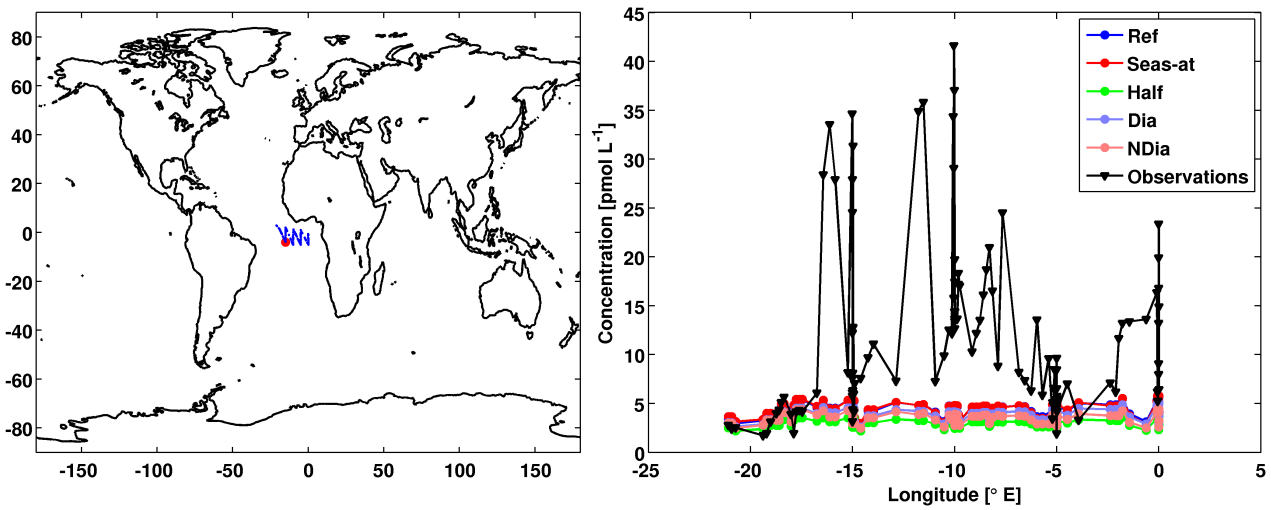

Figure S12 Observations are from the RV Maria S. Merian cruise MSM18/3 in June 2011 as listed in the SI of (Ziska et al., 2013).

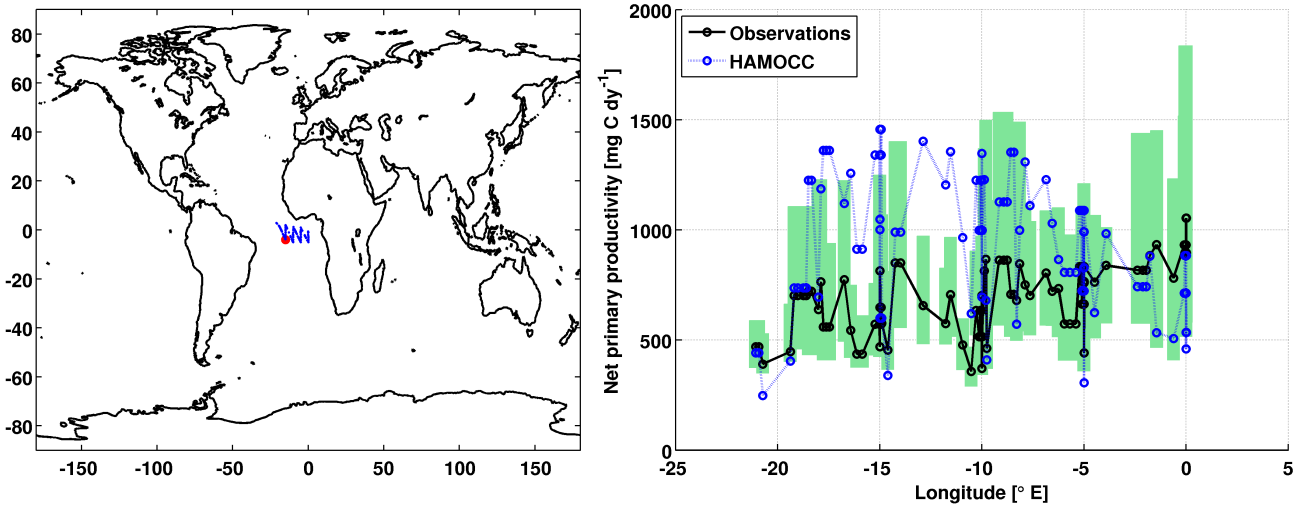

Figure S13 Simulated and observation-based net primary productivity [mg C m^{-2} dy^{-1}]. Green shades show mimimum and maximum range of the observation-based estimate, the black dashed line shows the median. The observation-based NPP product is based on data 1997-2009 from SeaWiFS Chl-*a*, PAR and AVHRR SST and derived using the VGPM model (Behrenfeld and Falkowski, 1997). The NPP producted was downloaded from http://wiki.icess.ucsb.edu/measures/NPP_Products (accessed June 2014).

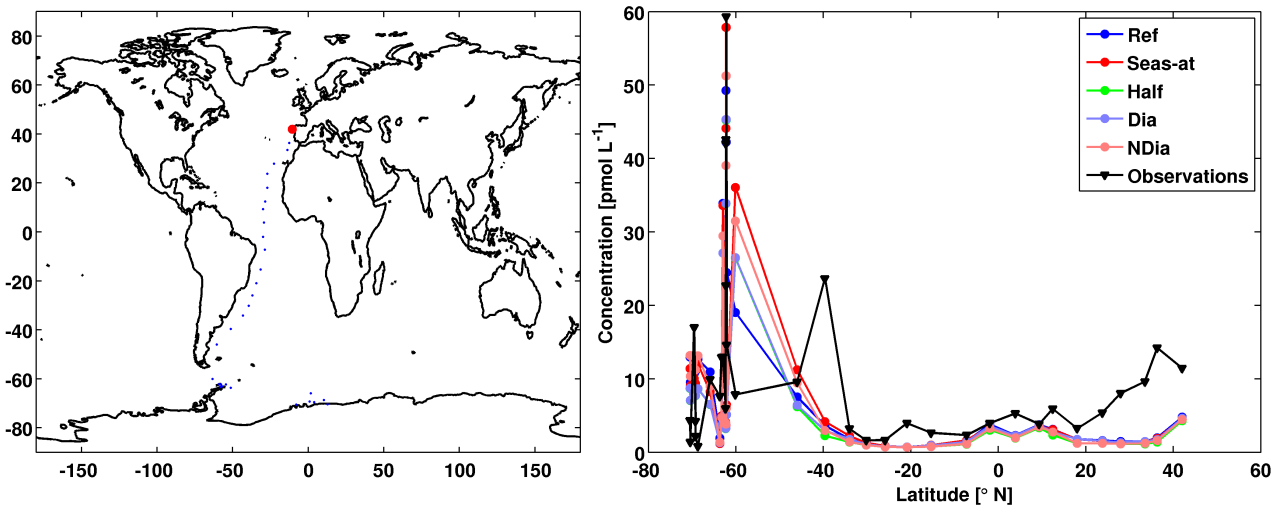

Figure S14 Observations are from the Polarstern cruise ANT X/1 in November 1994 (Schall et al., 1997) as listed in the SI of (Ziska et al., 2013).

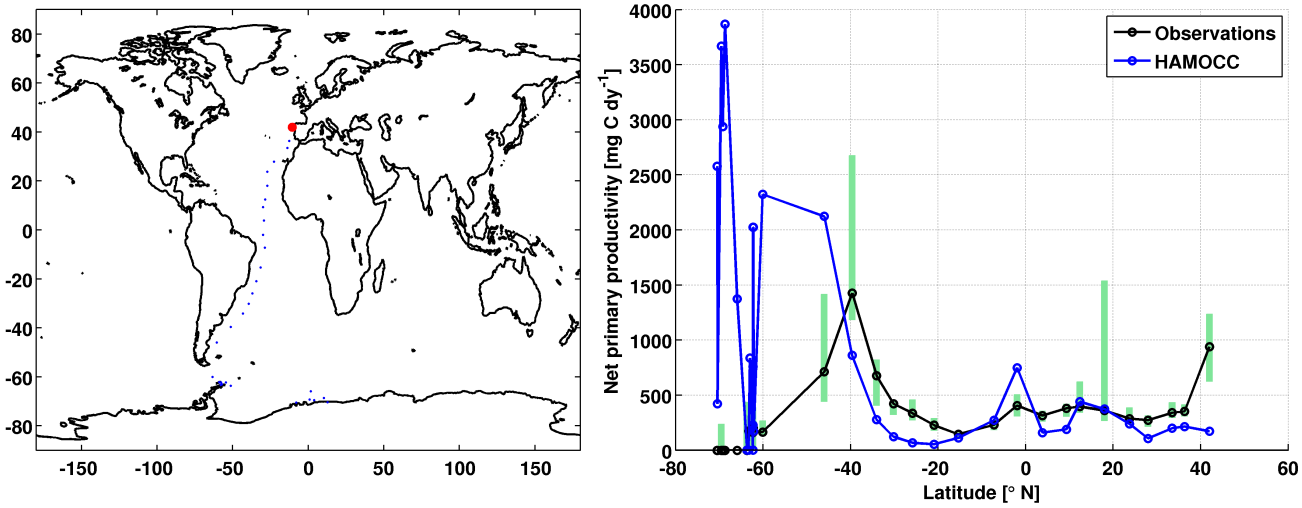

Figure S15 Simulated and observation-based net primary productivity [mg C m^{-2} dy^{-1}]. Green shades show mimimum and maximum range of the observation-based estimate, the black dashed line shows the median. The observation-based NPP product is based on data 1997-2009 from SeaWiFS Chl-*a*, PAR and AVHRR SST and derived using the VGPM model (Behrenfeld and Falkowski, 1997). The NPP producted was downloaded from http://wiki.icess.ucsb.edu/measures/NPP_Products (accessed June 2014).

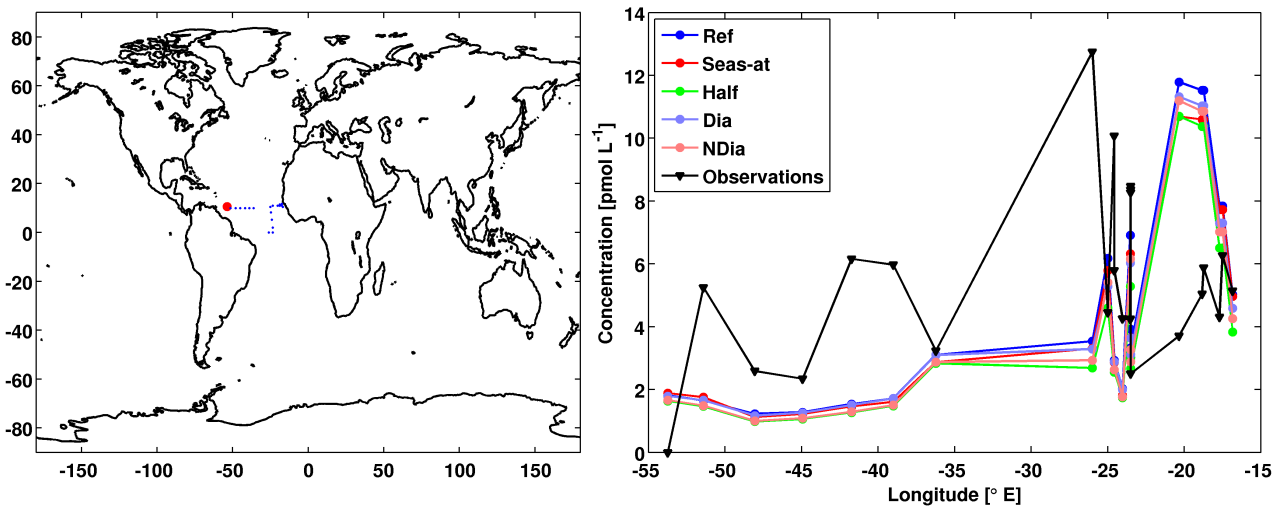

Figure S16 Observations are from the Meteor cruise M55, 12.10.-17.11.2002 (Quack et al., 2004) as listed in the SI of (Ziska et al., 2013).

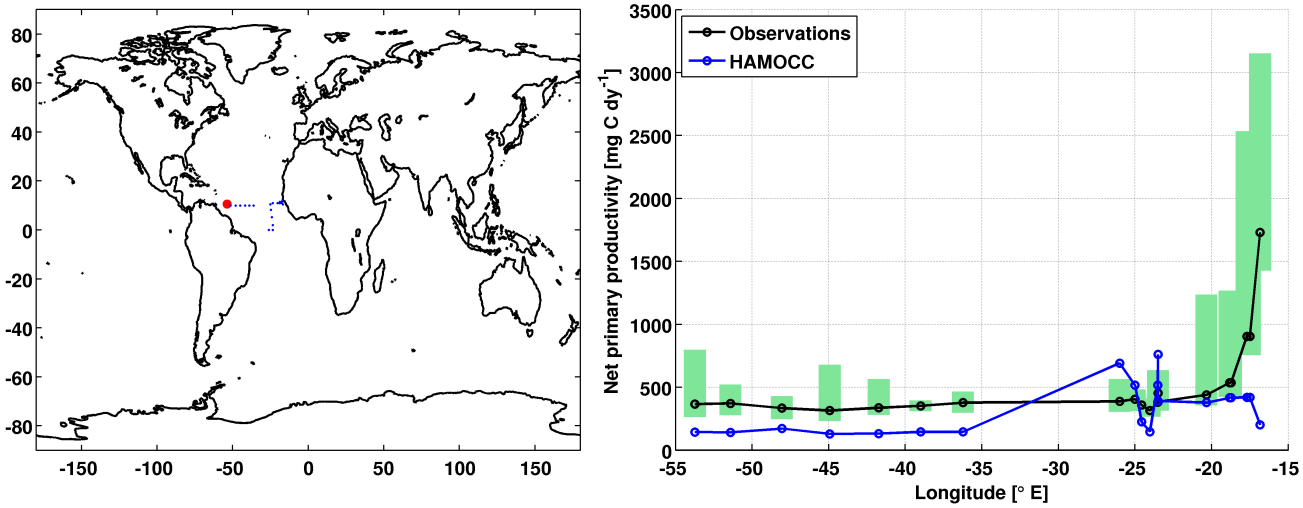

Figure S17 Simulated and observation-based net primary productivity [mg C m^{-2} dy^{-1}]. Green shades show mimimum and maximum range of the observation-based estimate, the black dashed line shows the median. The observation-based NPP product is based on data 1997-2009 from SeaWiFS Chl-*a*, PAR and AVHRR SST and derived using the VGPM model (Behrenfeld and Falkowski, 1997). The NPP producted was downloaded from http://wiki.icess.ucsb.edu/measures/NPP_Products (accessed June 2014).

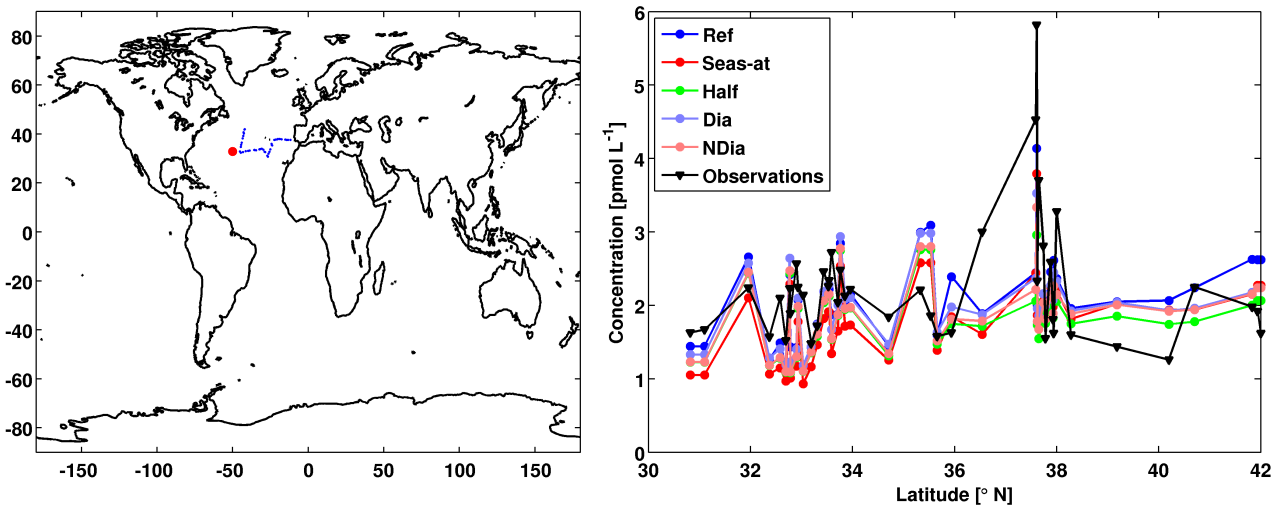

Figure S18 Observations are from the Meteor cruise M60_5, 09.03.-15.04.2004 as listed in the SI of (Ziska et al., 2013).

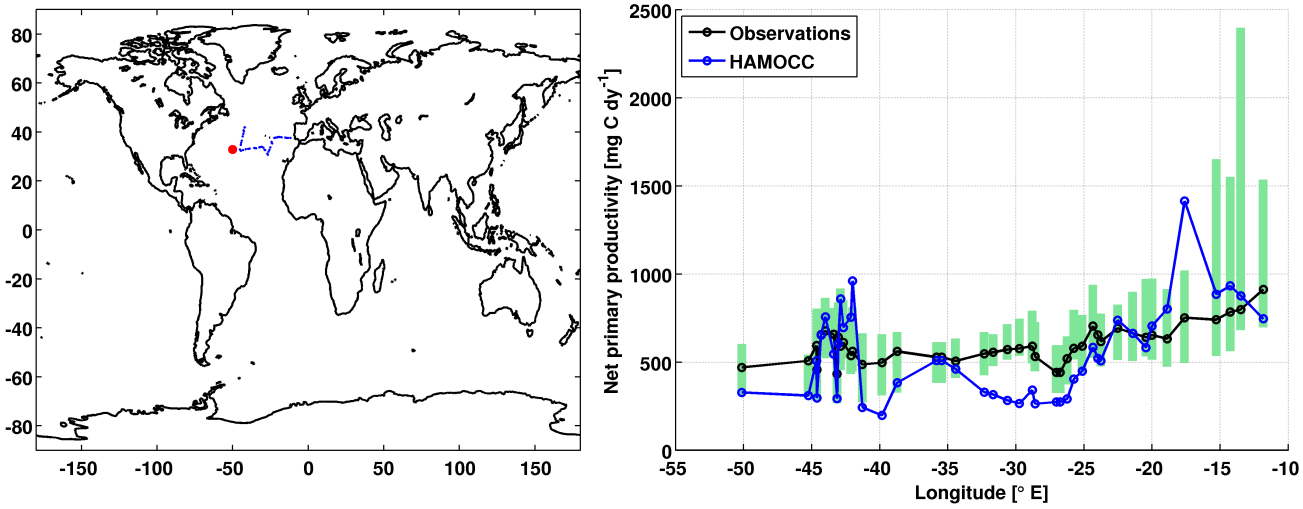

Figure S19 Simulated and observation-based net primary productivity [mg C m^{-2} dy^{-1}]. Green shades show mimimum and maximum range of the observation-based estimate, the black dashed line shows the median. The observation-based NPP product is based on data 1997-2009 from SeaWiFS Chl-*a*, PAR and AVHRR SST and derived using the VGPM model (Behrenfeld and Falkowski, 1997). The NPP producted was downloaded from http://wiki.icess.ucsb.edu/measures/NPP_Products (accessed June 2014).

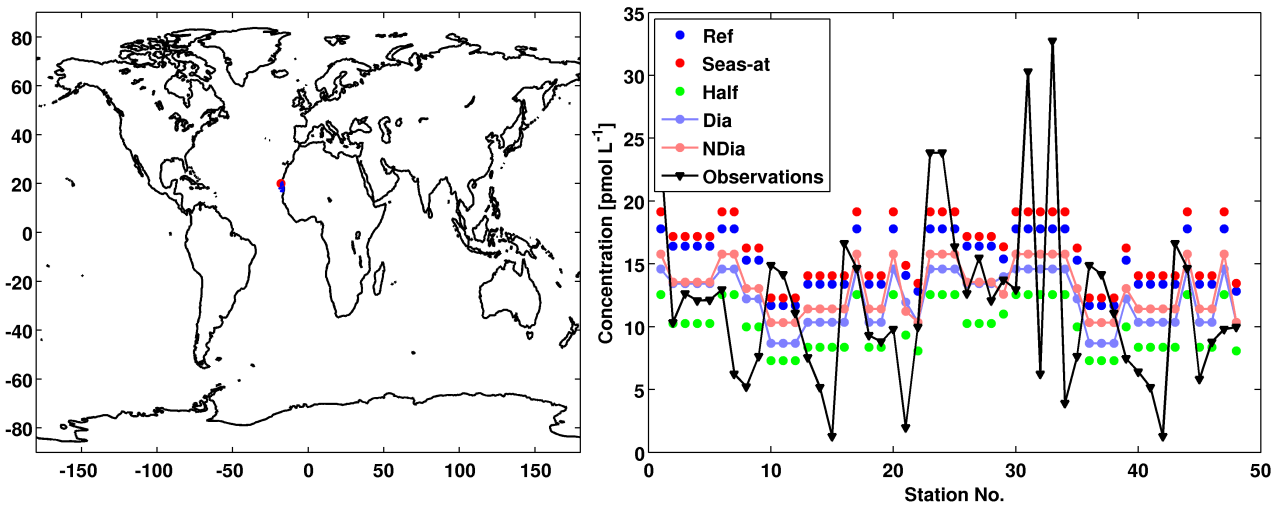

Figure S20 Observations are from the Poseidon cruise 320_1, 21.03.-07.04.2005 (Quack et al., 2007) as listed in the SI of (Ziska et al., 2013).

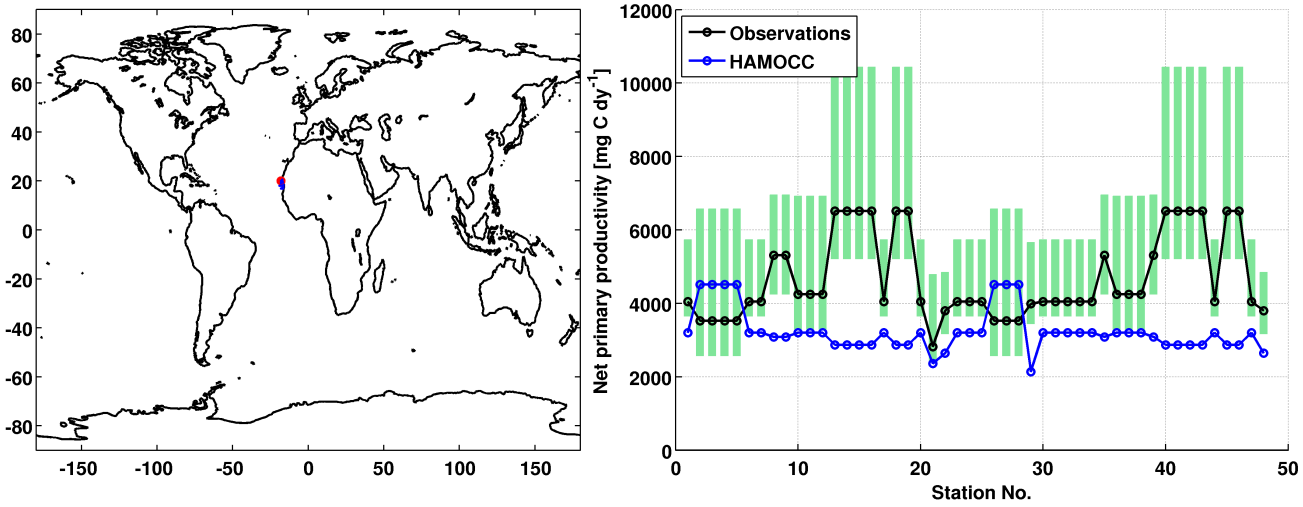

Figure S21 Simulated and observation-based net primary productivity [mg C m^{-2} dy^{-1}]. Green shades show mimimum and maximum range of the observation-based estimate, the black dashed line shows the median. The observation-based NPP product is based on data 1997-2009 from SeaWiFS Chl-*a*, PAR and AVHRR SST and derived using the VGPM model (Behrenfeld and Falkowski, 1997). The NPP producted was downloaded from http://wiki.icess.ucsb.edu/measures/NPP_Products (accessed June 2014).

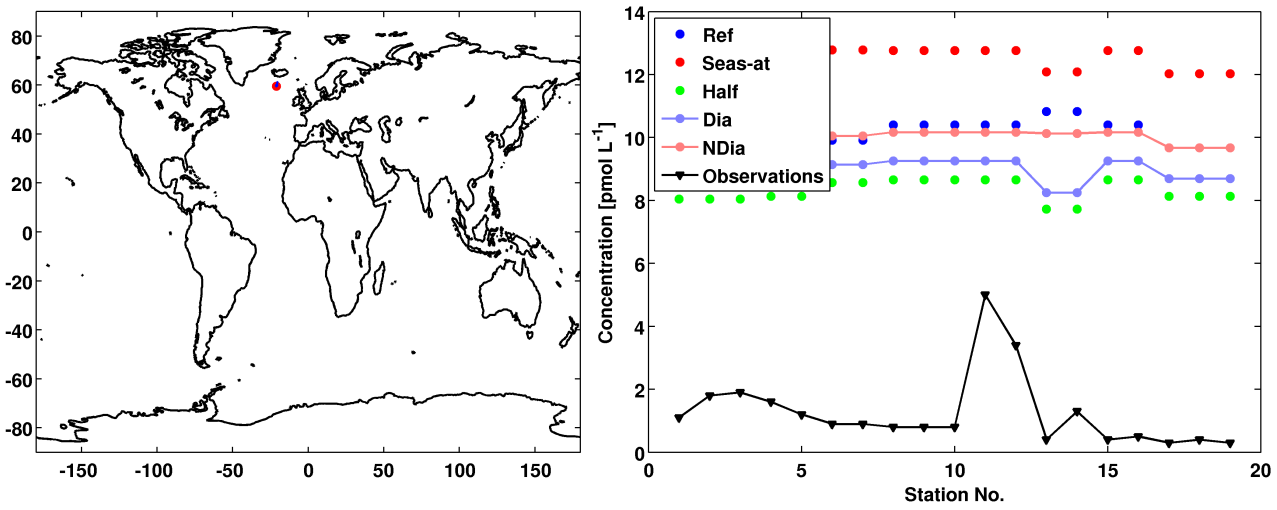

Figure S22 Observations are from the Discovery cruise ASCOE in June 1998 (Baker et al., 1999) as listed in the SI of (Ziska et al., 2013).

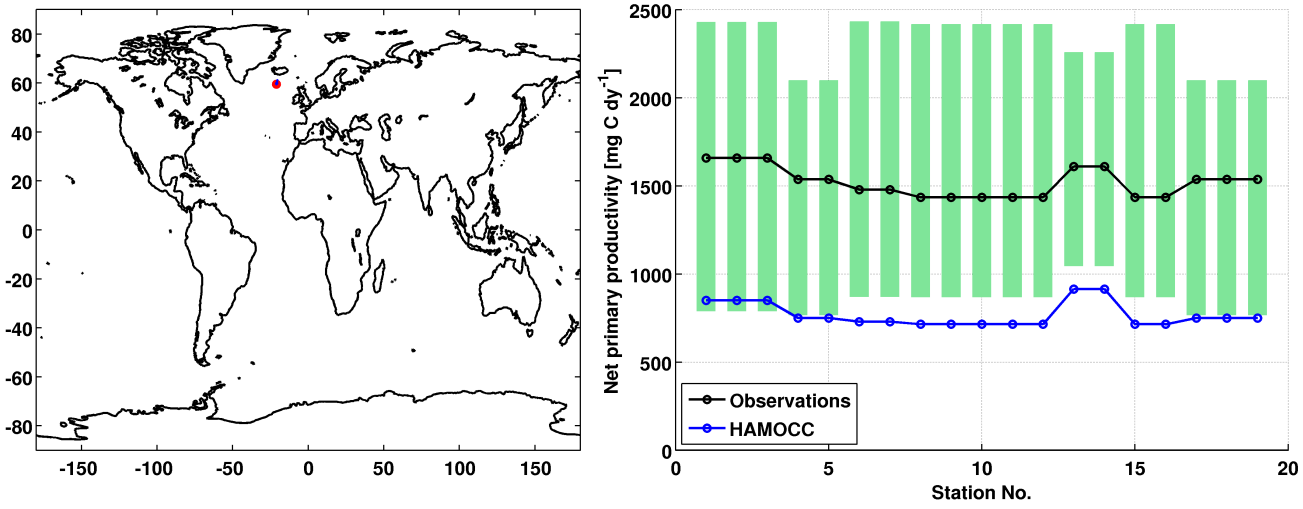

Figure S23 Simulated and observation-based net primary productivity [mg C m^{-2} dy^{-1}]. Green shades show mimimum and maximum range of the observation-based estimate, the black dashed line shows the median. The observation-based NPP product is based on data 1997-2009 from SeaWiFS Chl-*a*, PAR and AVHRR SST and derived using the VGPM model (Behrenfeld and Falkowski, 1997). The NPP producted was downloaded from http://wiki.icess.ucsb.edu/measures/NPP_Products (accessed June 2014).

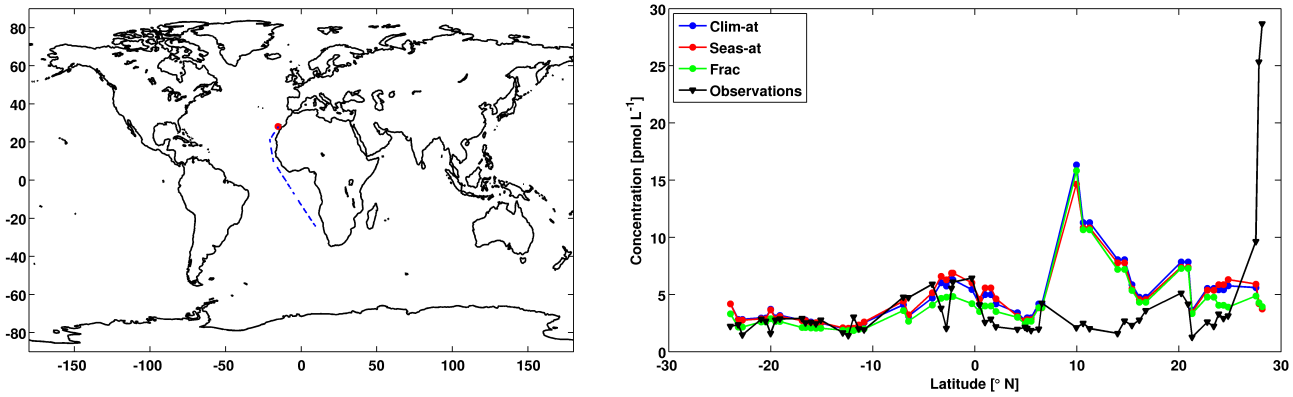

Figure S24 Observations are from the Polarstern cruise ANT XVII/1 in August 2000 (Chuck et al., 2005) as listed in the SI of (Ziska et al., 2013).

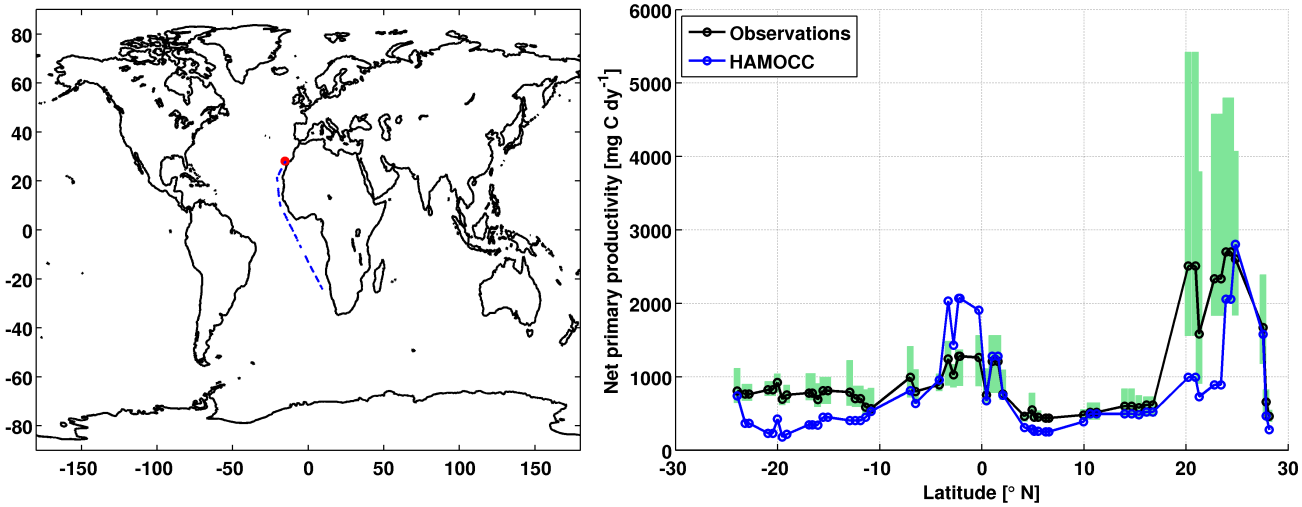

Figure S25 Simulated and observation-based net primary productivity [mg C m^{-2} dy^{-1}]. Green shades show mimimum and maximum range of the observation-based estimate, the black dashed line shows the median. The observation-based NPP product is based on data 1997-2009 from SeaWiFS Chl-*a*, PAR and AVHRR SST and derived using the VGPM model (Behrenfeld and Falkowski, 1997). The NPP producted was downloaded from http://wiki.icess.ucsb.edu/measures/NPP_Products (accessed June 2014).

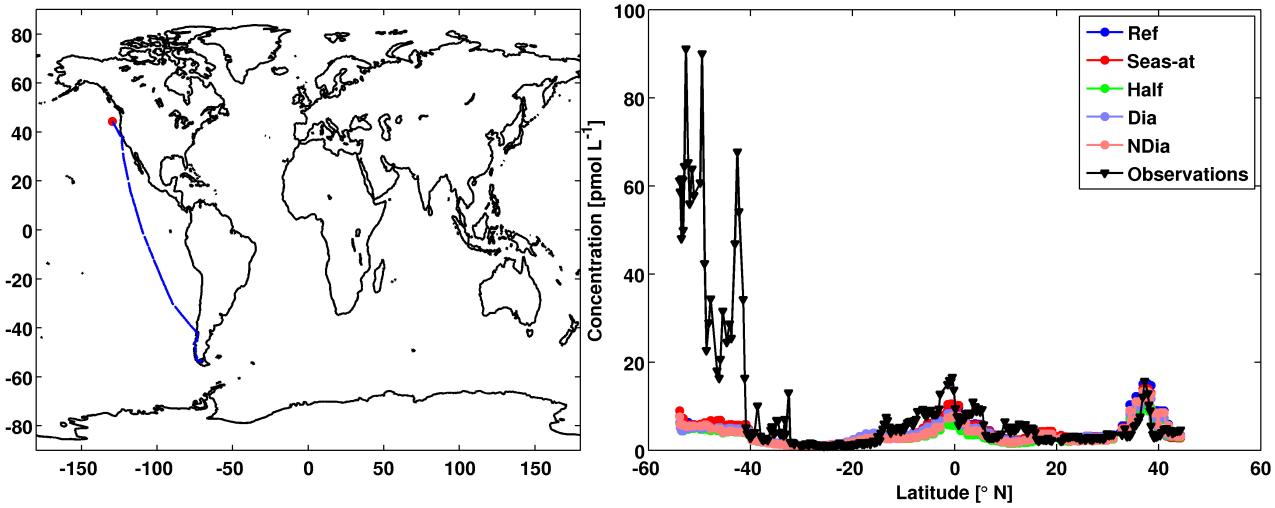

Figure S26 Observations are from the Discoverer cruise BLAST 1, 18.01.-17.02.1994 (Butler et al., 2007) as listed in the SI of (Ziska et al., 2013).

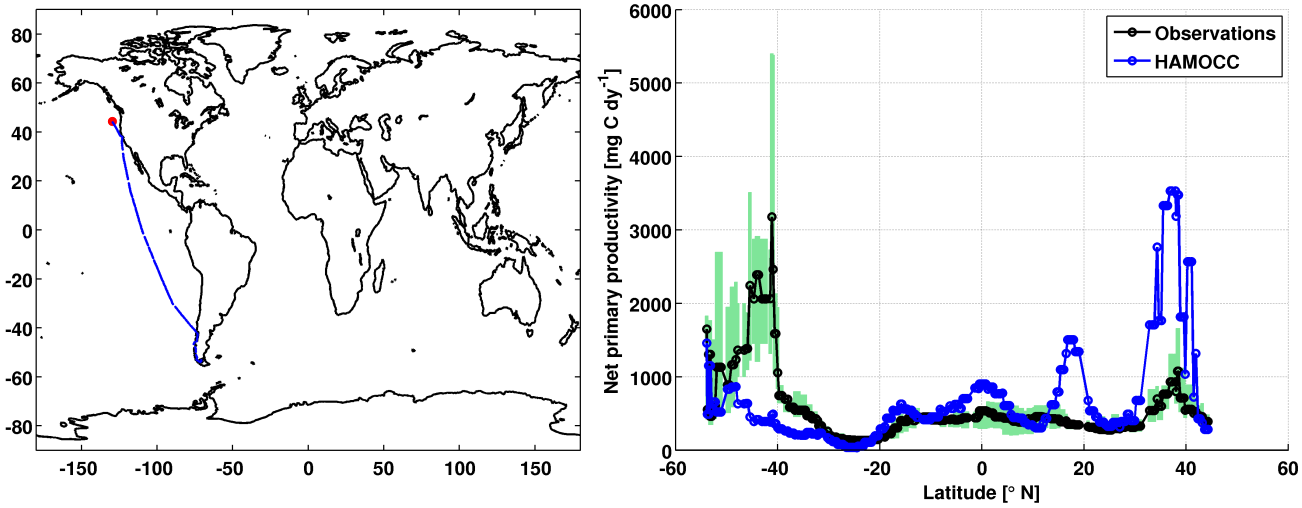

Figure S27 Simulated and observation-based net primary productivity [mg C m^{-2} dy^{-1}]. Green shades show mimimum and maximum range of the observation-based estimate, the black dashed line shows the median. The observation-based NPP product is based on data 1997-2009 from SeaWiFS Chl-*a*, PAR and AVHRR SST and derived using the VGPM model (Behrenfeld and Falkowski, 1997). The NPP producted was downloaded from http://wiki.icess.ucsb.edu/measures/NPP_Products (accessed June 2014).

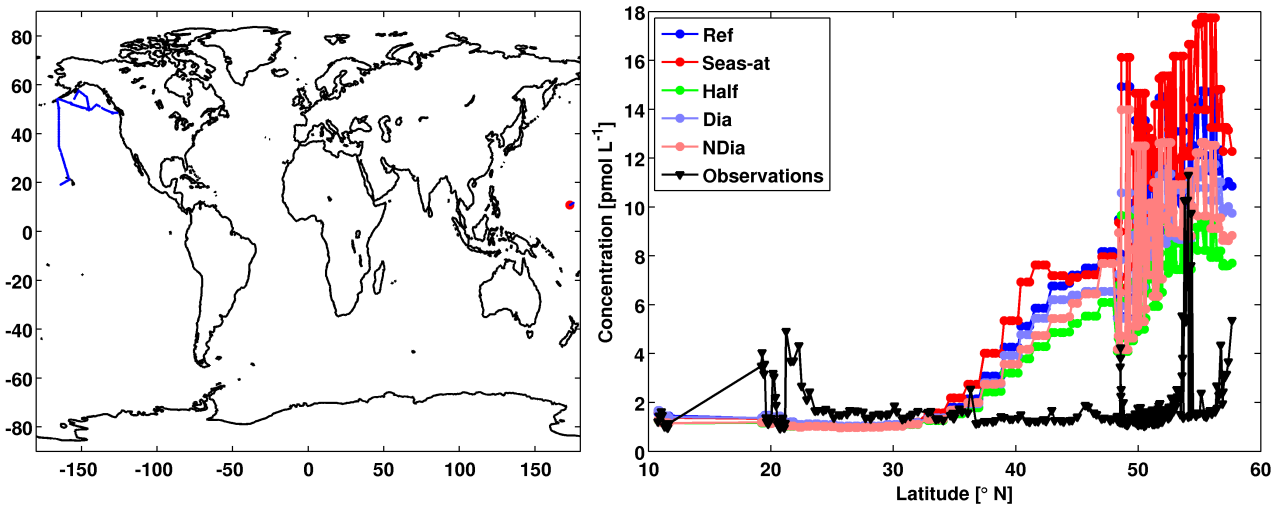

Figure S28 Observations are from the NOAA ship Ronald H. Brown cruise Gas Ex 98, 07.05.-27.07.1998 (Butler et al., 2007) as listed in the SI of (Ziska et al., 2013).

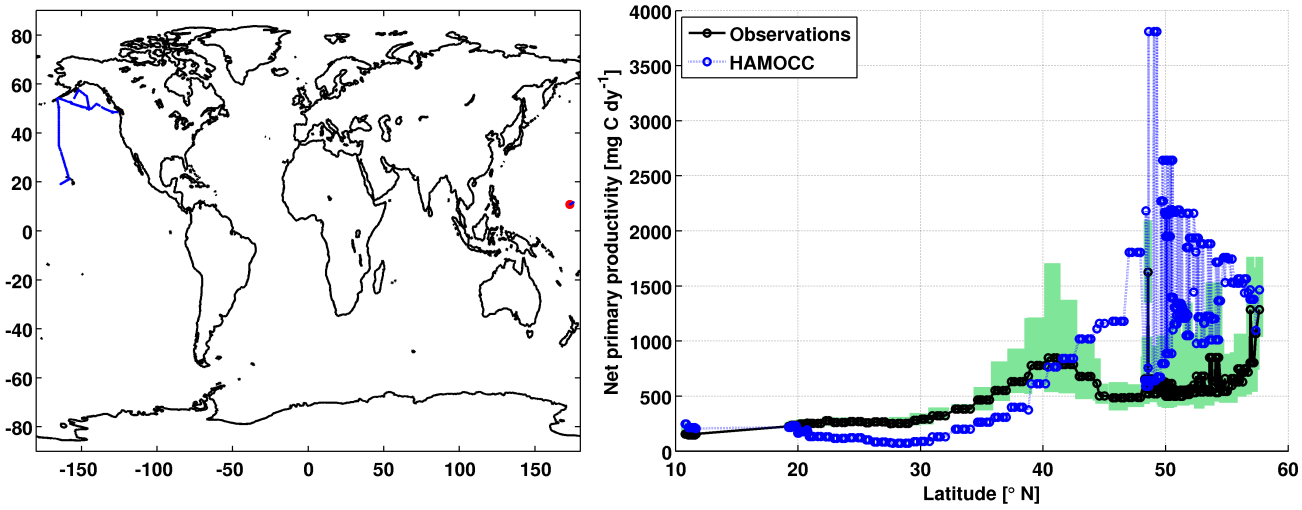

Figure S29 Simulated and observation-based net primary productivity [mg C m^{-2} dy^{-1}]. Green shades show mimimum and maximum range of the observation-based estimate, the black dashed line shows the median. The observation-based NPP product is based on data 1997-2009 from SeaWiFS Chl-*a*, PAR and AVHRR SST and derived using the VGPM model (Behrenfeld and Falkowski, 1997). The NPP producted was downloaded from http://wiki.icess.ucsb.edu/measures/NPP_Products (accessed June 2014).

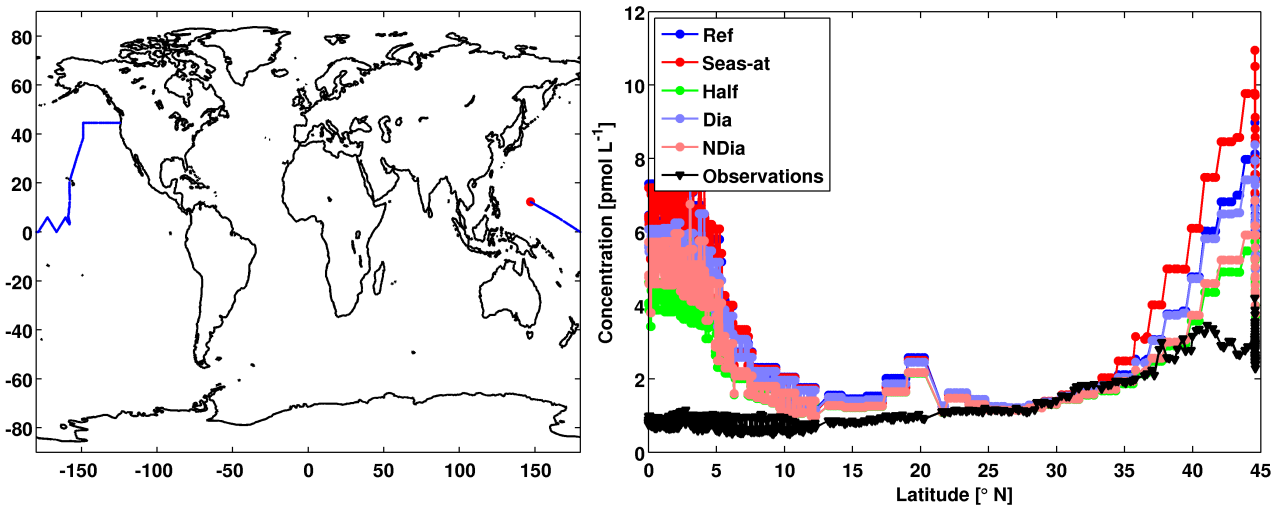

Figure S30 Observations are from the R/V Wecoma cruise Phase 1-04, 22.5.-02.07.2004 (Butler et al., 2007) as listed in the SI of (Ziska et al., 2013).

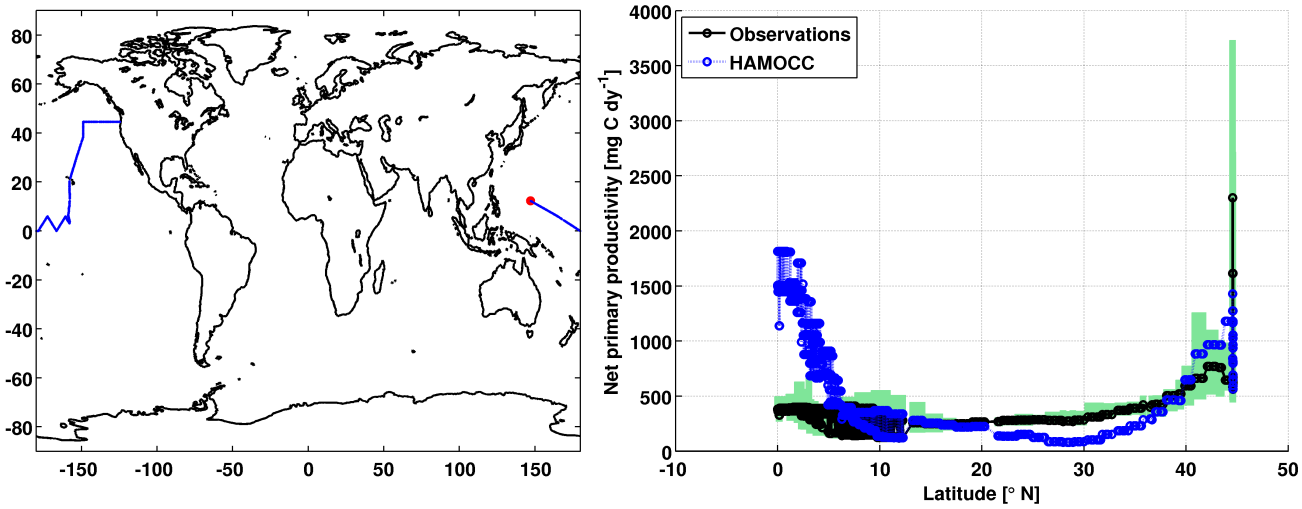

Figure S31 Simulated and observation-based net primary productivity [mg C m^{-2} dy^{-1}]. Green shades show mimimum and maximum range of the observation-based estimate, the black dashed line shows the median. The observation-based NPP product is based on data 1997-2009 from SeaWiFS Chl-*a*, PAR and AVHRR SST and derived using the VGPM model (Behrenfeld and Falkowski, 1997). The NPP producted was downloaded from http://wiki.icess.ucsb.edu/measures/NPP_Products (accessed June 2014).

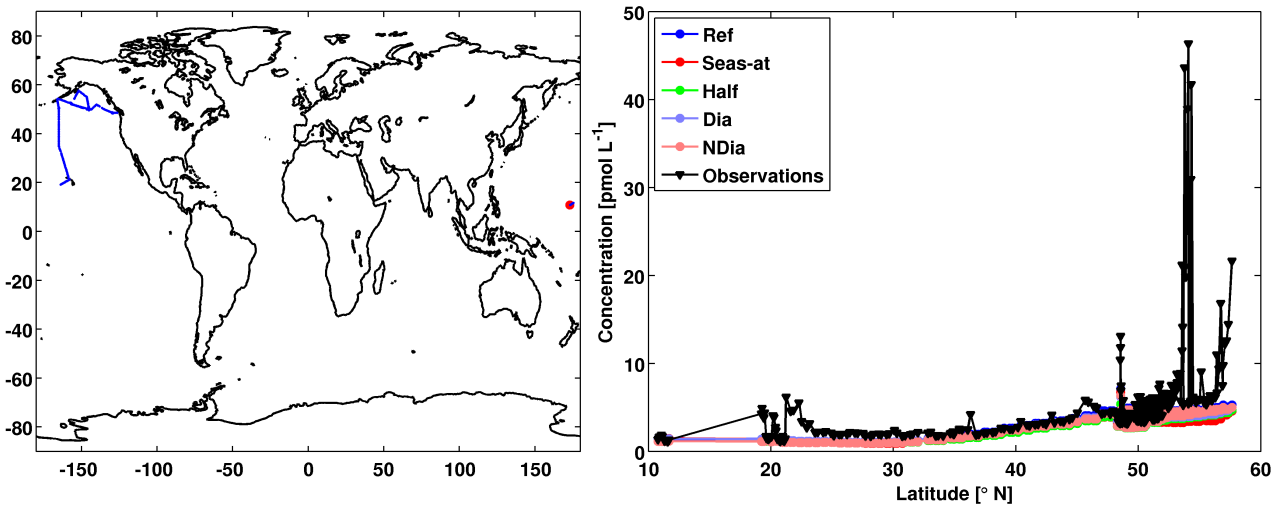

Figure S32 Observations are from the NOAA ship Ronald H. Brown cruise RB-99-06, 14.09.-23.10.1999 (Butler et al., 2007) as listed in the SI of (Ziska et al., 2013).

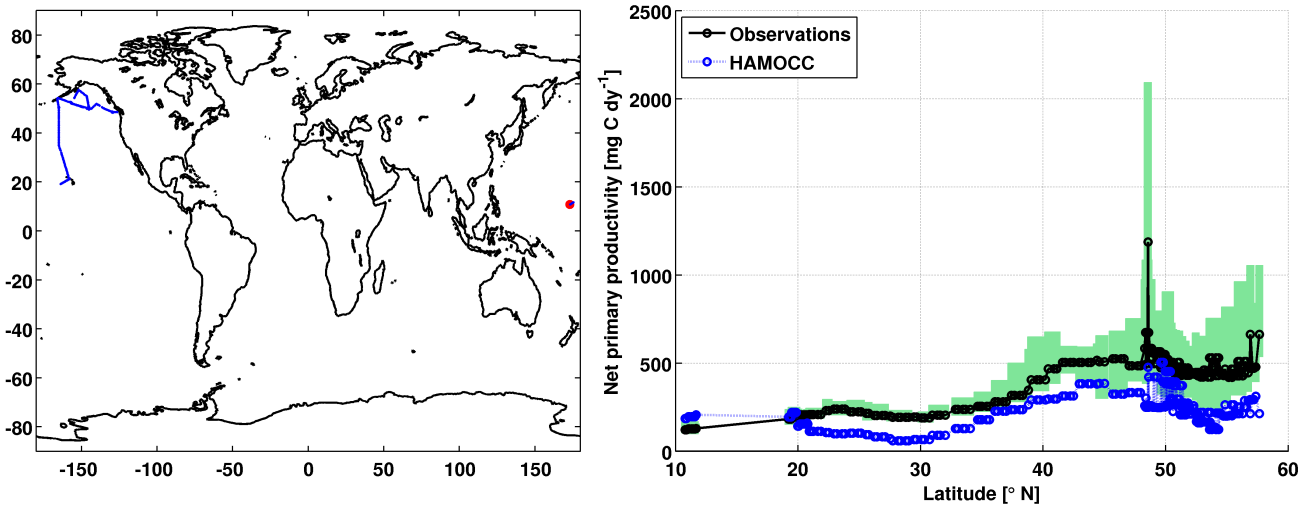

Figure S33 Simulated and observation-based net primary productivity [mg C m^{-2} dy^{-1}]. Green shades show mimimum and maximum range of the observation-based estimate, the black dashed line shows the median. The observation-based NPP product is based on data 1997-2009 from SeaWiFS Chl-*a*, PAR and AVHRR SST and derived using the VGPM model (Behrenfeld and Falkowski, 1997). The NPP producted was downloaded from http://wiki.icess.ucsb.edu/measures/NPP_Products (accessed June 2014).

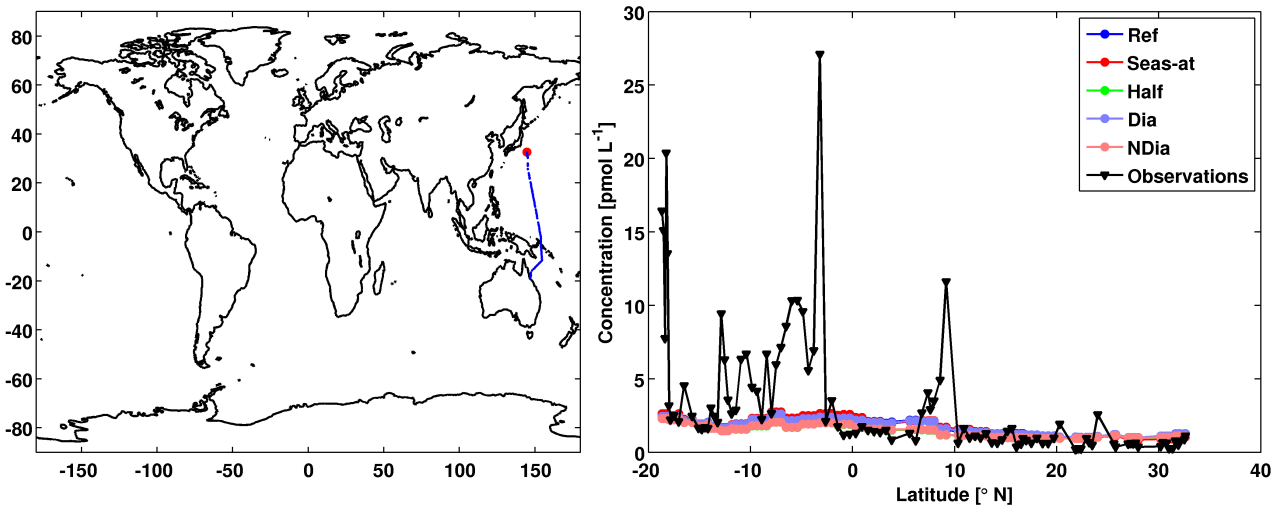

Figure S34 Observations are from the R/V Sonne cruise TransBrom Sonne in Oktober 2009 as listed in the SI of (Ziska et al., 2013).

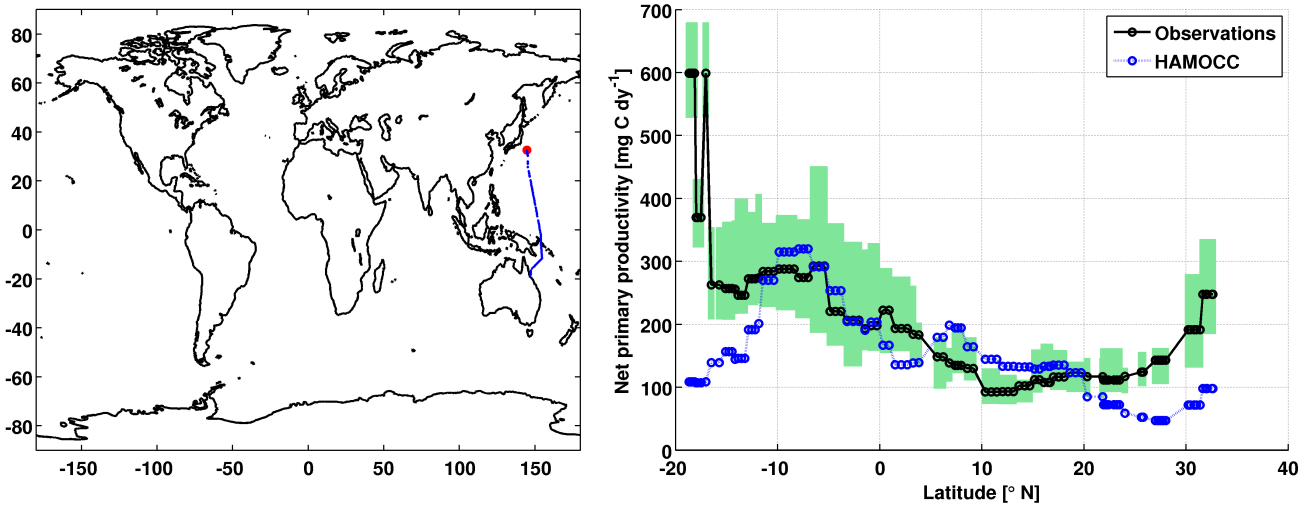

Figure S35 Simulated and observation-based net primary productivity [mg C m^{-2} dy^{-1}]. Green shades show mimimum and maximum range of the observation-based estimate, the black dashed line shows the median. The observation-based NPP product is based on data 1997-2009 from SeaWiFS Chl-*a*, PAR and AVHRR SST and derived using the VGPM model (Behrenfeld and Falkowski, 1997). The NPP producted was downloaded from http://wiki.icess.ucsb.edu/measures/NPP_Products (accessed June 2014).

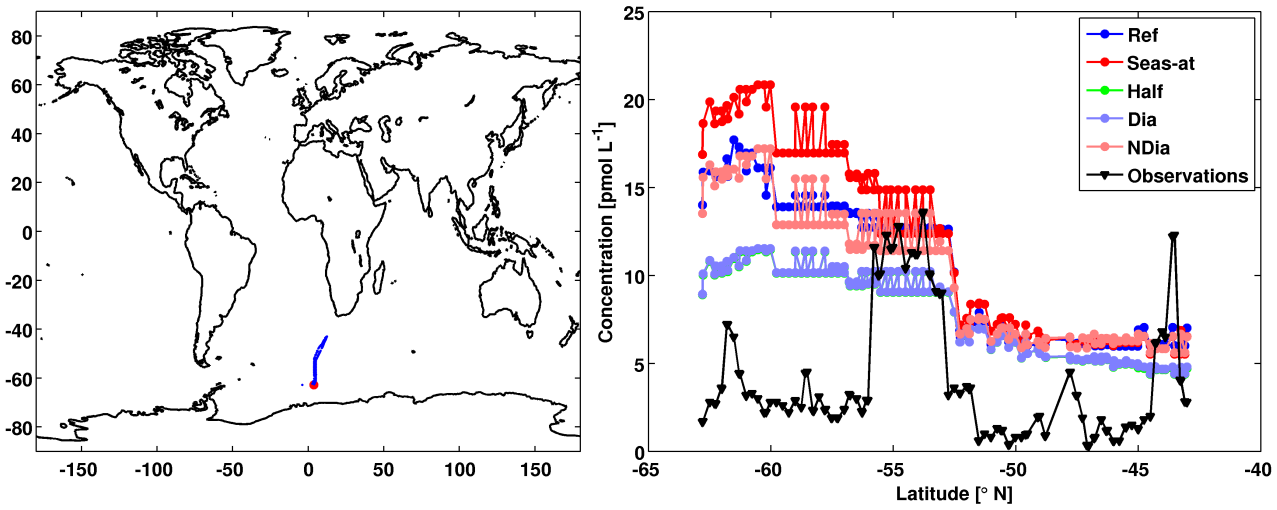

Figure S36 Observations are from the SA Agulhas cruise SWEDARP_97/98 in December 1997 (Abrahamsson et al., 2004) as listed in the SI of (Ziska et al., 2013).

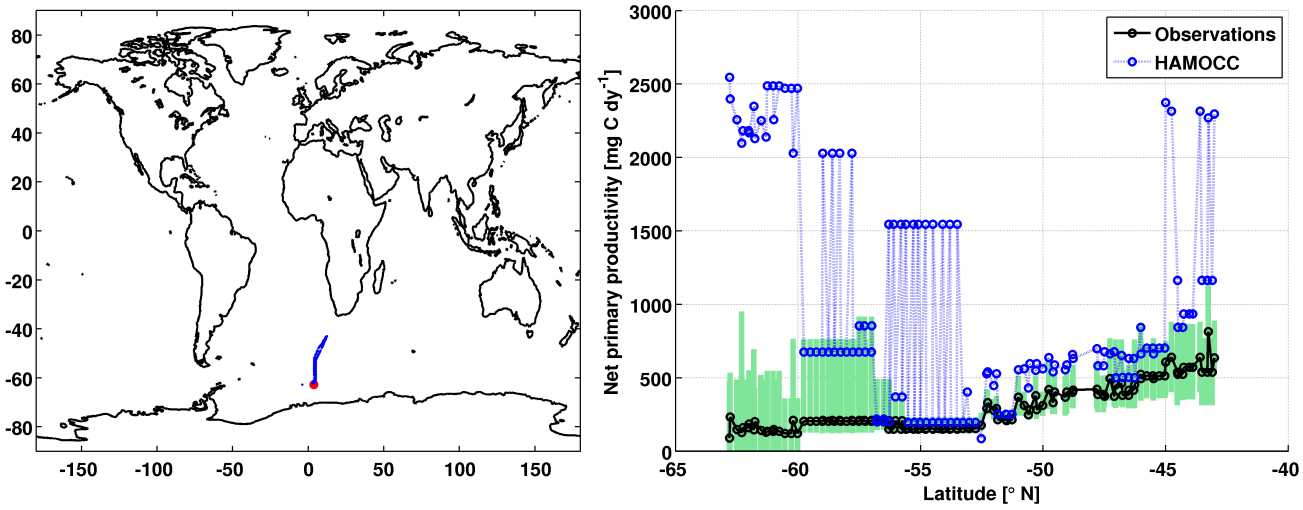

Figure S37 Simulated and observation-based net primary productivity [mg C m^{-2} dy^{-1}]. Green shades show mimimum and maximum range of the observation-based estimate, the black dashed line shows the median. The observation-based NPP product is based on data 1997-2009 from SeaWiFS Chl-*a*, PAR and AVHRR SST and derived using the VGPM model (Behrenfeld and Falkowski, 1997). The NPP producted was downloaded from http://wiki.icess.ucsb.edu/measures/NPP_Products (accessed June 2014).

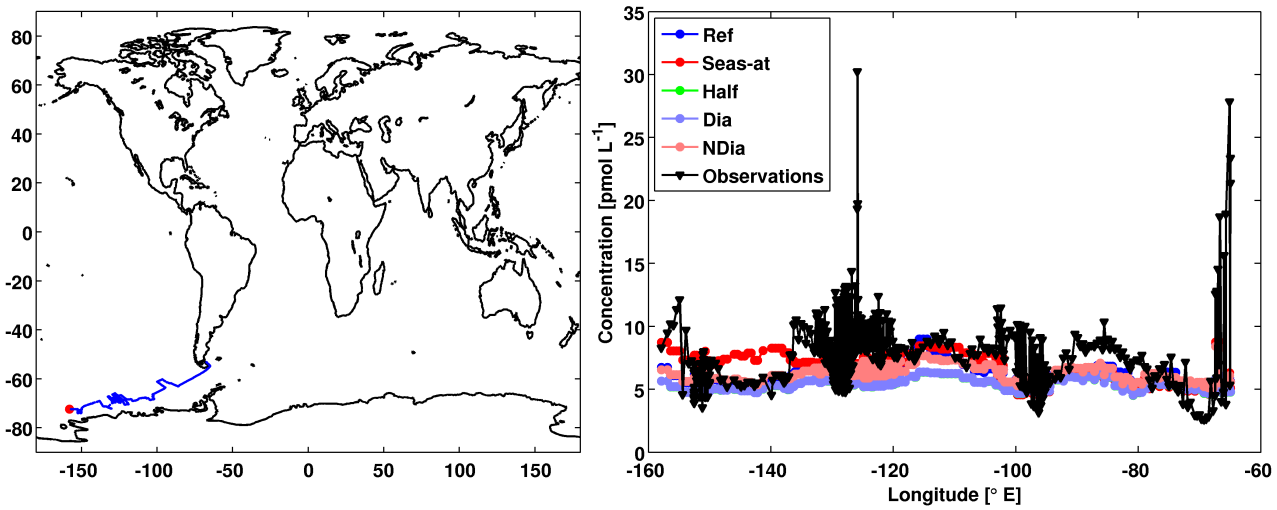

Figure S38 Observations are from the Nathaniel B. Palmer cruise BLAST 3, 22.02.-07.04.1996 (Butler et al., 2007) as listed in the SI of (Ziska et al., 2013).

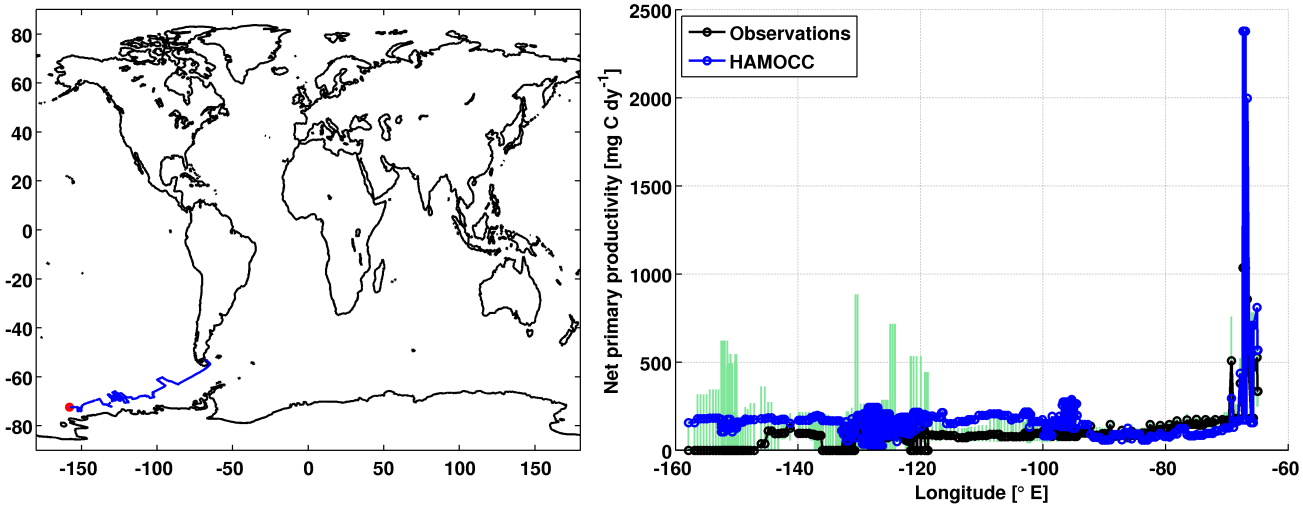

Figure S39 Simulated and observation-based net primary productivity [mg C m^{-2} dy^{-1}]. Green shades show mimimum and maximum range of the observation-based estimate, the black dashed line shows the median. The observation-based NPP product is based on data 1997-2009 from SeaWiFS Chl-*a*, PAR and AVHRR SST and derived using the VGPM model (Behrenfeld and Falkowski, 1997). The NPP producted was downloaded from http://wiki.icess.ucsb.edu/measures/NPP_Products (accessed June 2014).

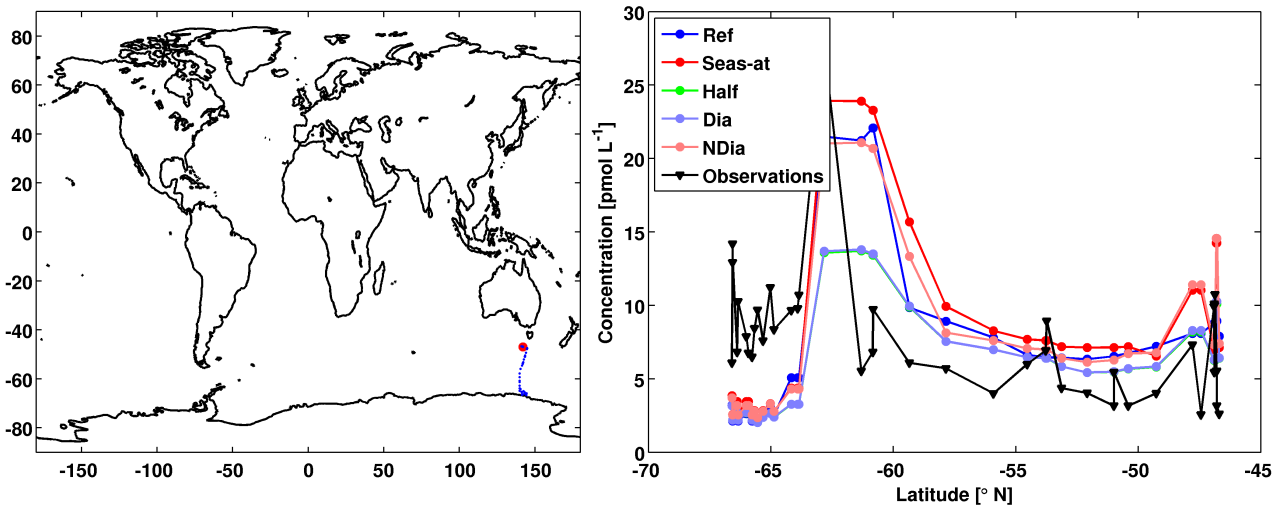

Figure S40 Observations are from the Aurora Australis cruise CLIVAR01, 29.10.-13.12. 2001 (Butler et al., 2007) as listed in the SI of (Ziska et al., 2013).

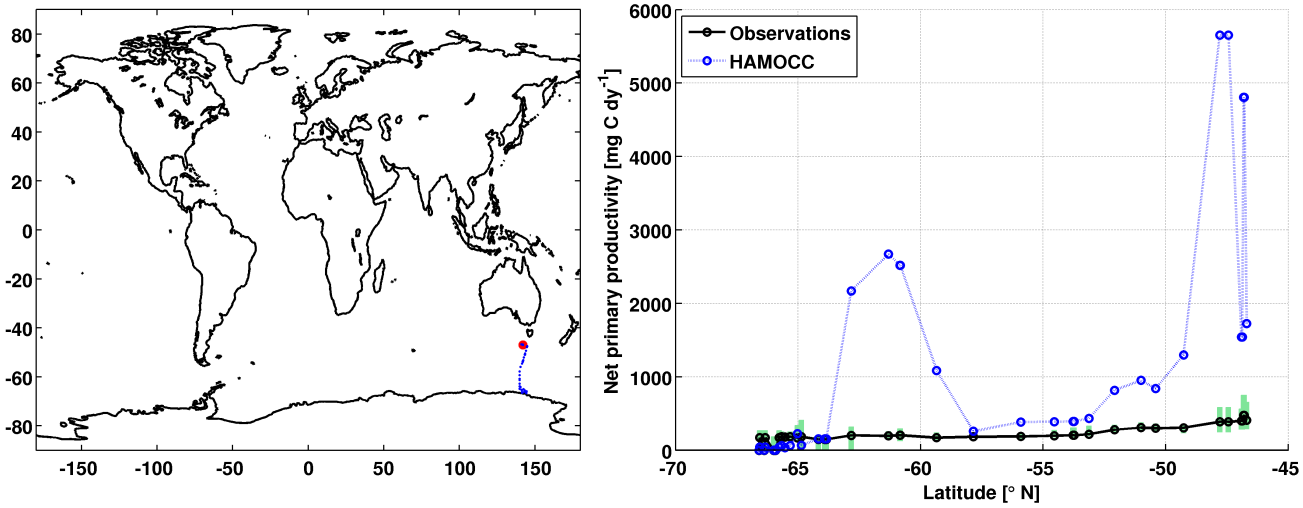

Figure S41 Simulated and observation-based net primary productivity [mg C m^{-2} dy^{-1}]. Green shades show mimimum and maximum range of the observation-based estimate, the black dashed line shows the median. The observation-based NPP product is based on data 1997-2009 from SeaWiFS Chl-*a*, PAR and AVHRR SST and derived using the VGPM model (Behrenfeld and Falkowski, 1997). The NPP producted was downloaded from http://wiki.icess.ucsb.edu/measures/NPP_Products (accessed June 2014).

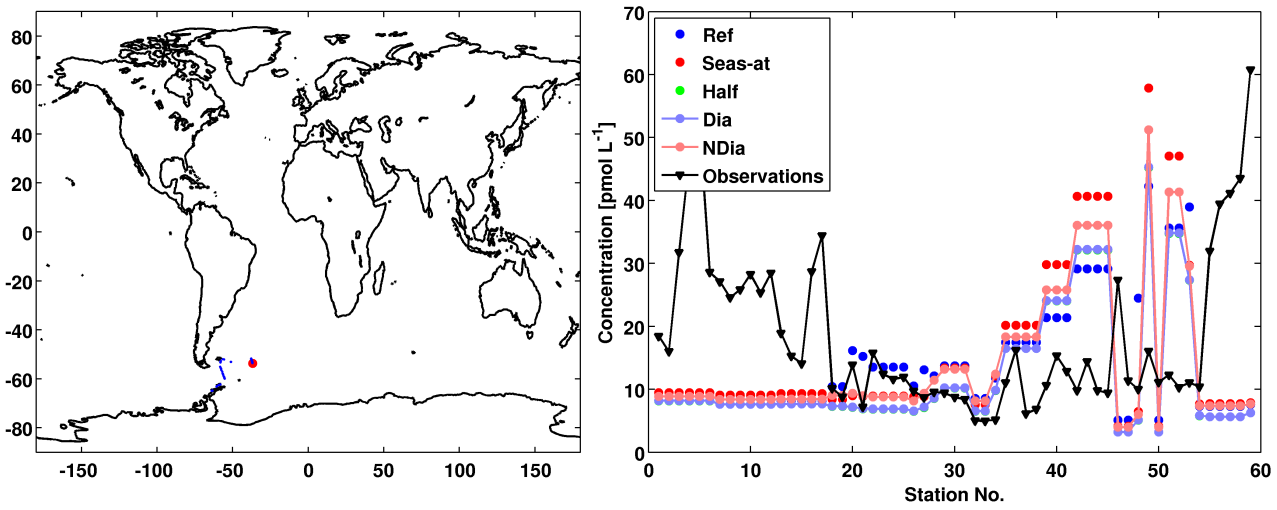

Figure S42 Observations are from the James Clark Ross cruise SAMS northen seas program (JR75) in November 2004 as listed in the SI of (Ziska et al., 2013).

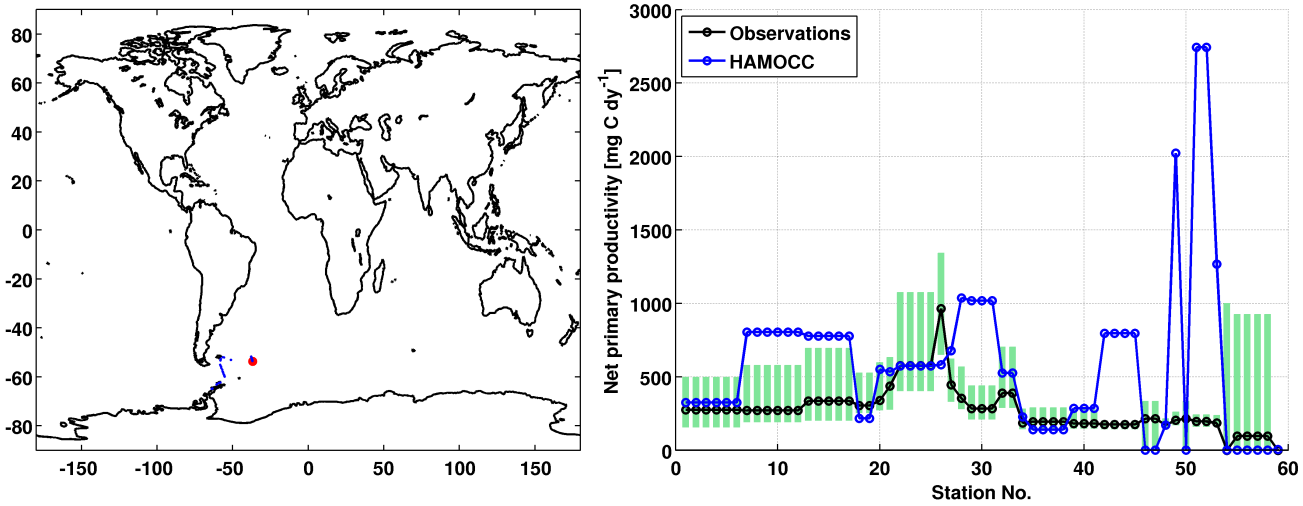

Figure S43 Simulated and observation-based net primary productivity [mg C m^{-2} dy^{-1}]. Green shades show mimimum and maximum range of the observation-based estimate, the black dashed line shows the median. The observation-based NPP product is based on data 1997-2009 from SeaWiFS Chl-*a*, PAR and AVHRR SST and derived using the VGPM model (Behrenfeld and Falkowski, 1997). The NPP producted was downloaded from http://wiki.icess.ucsb.edu/measures/NPP_Products (accessed June 2014).

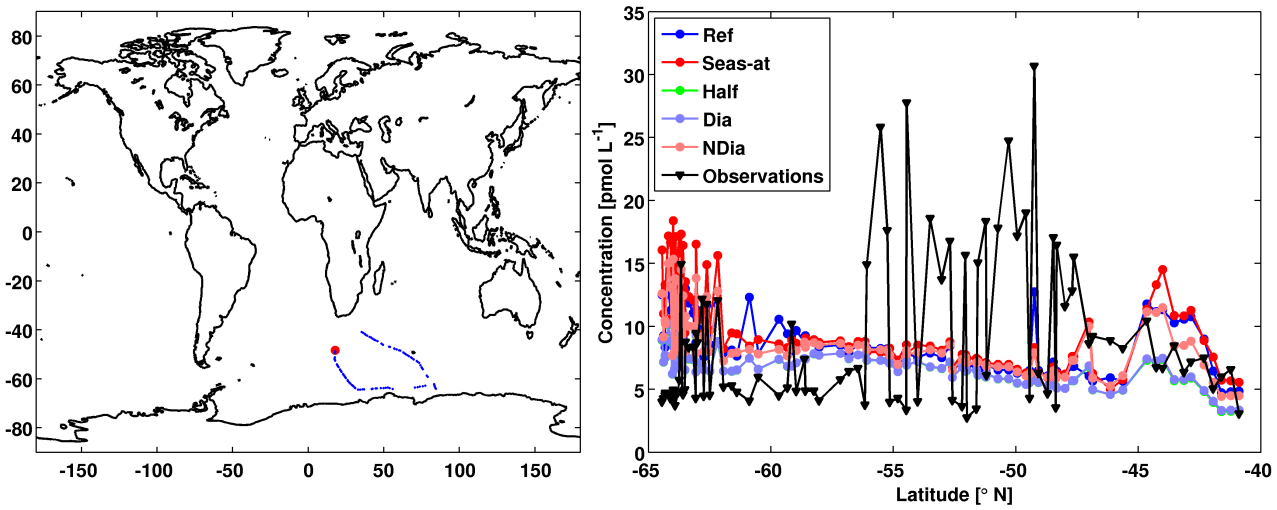

Figure S44 Observations are from the RRS Discovery (DISCO 200) cruise ADOX (Atlantic Deep Outflow Experiment) in February 1993 (Chuck et al., 2005) as listed in the SI of (Ziska et al., 2013).

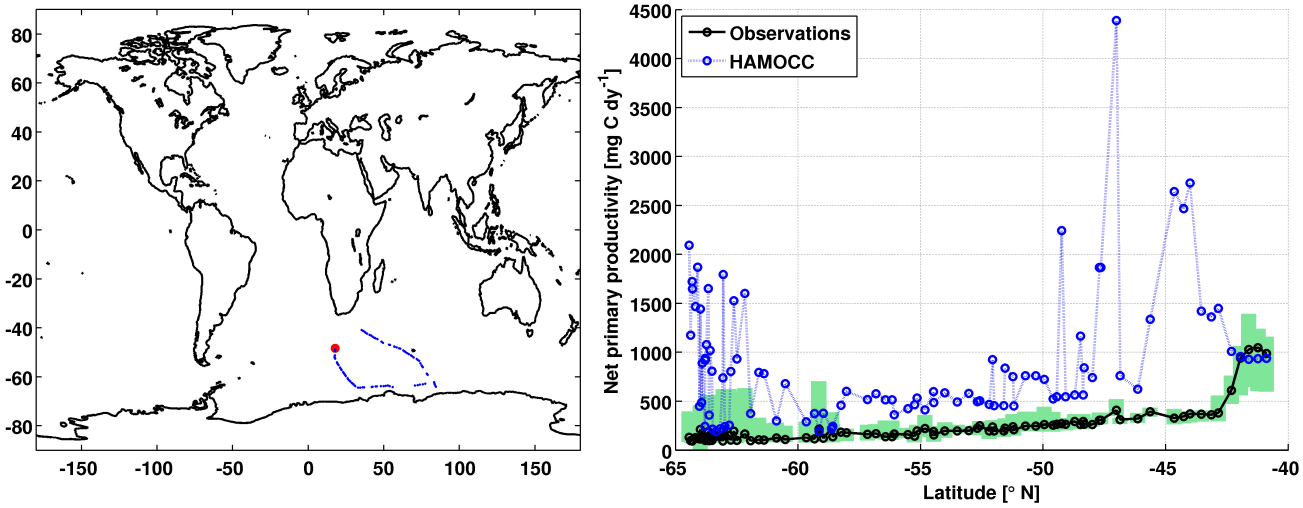

Figure S45 Simulated and observation-based net primary productivity [mg C m^{-2} dy^{-1}]. Green shades show mimimum and maximum range of the observation-based estimate, the black dashed line shows the median. The observation-based NPP product is based on data 1997-2009 from SeaWiFS Chl-*a*, PAR and AVHRR SST and derived using the VGPM model (Behrenfeld and Falkowski, 1997). The NPP producted was downloaded from http://wiki.icess.ucsb.edu/measures/NPP_Products (accessed June 2014).

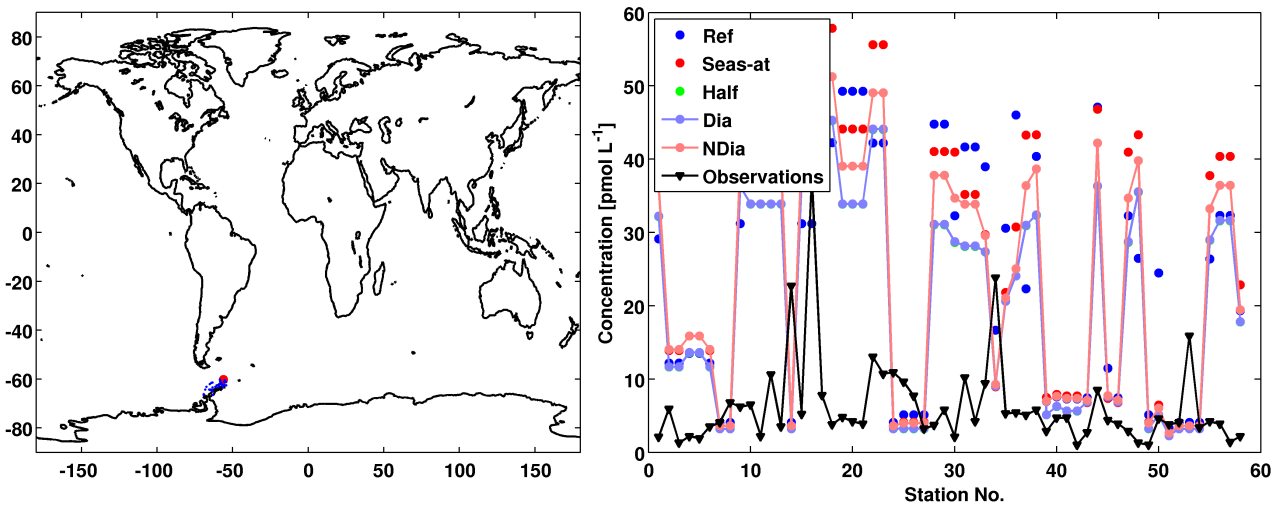

Figure S46 Observations are from the Polarstern cruise ANT VI/2 in November 1987 as listed in the SI of (Ziska et al., 2013).

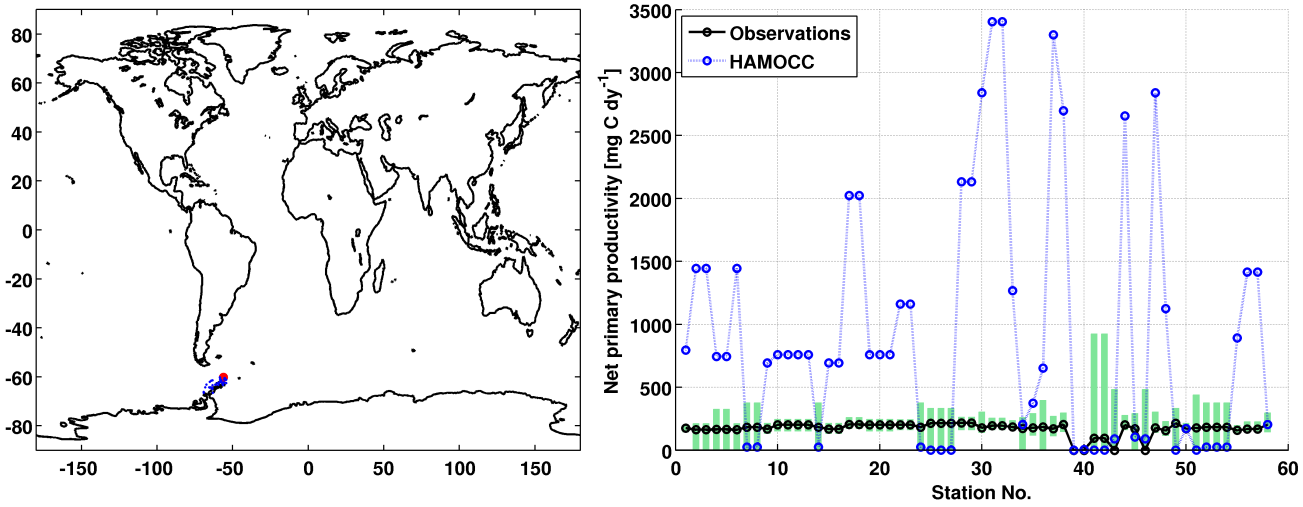

Figure S47 Simulated and observation-based net primary productivity [mg C m^{-2} dy^{-1}]. Green shades show mimimum and maximum range of the observation-based estimate, the black dashed line shows the median. The observation-based NPP product is based on data 1997-2009 from SeaWiFS Chl-*a*, PAR and AVHRR SST and derived using the VGPM model (Behrenfeld and Falkowski, 1997). The NPP producted was downloaded from http://wiki.icess.ucsb.edu/measures/NPP_Products (accessed June 2014).

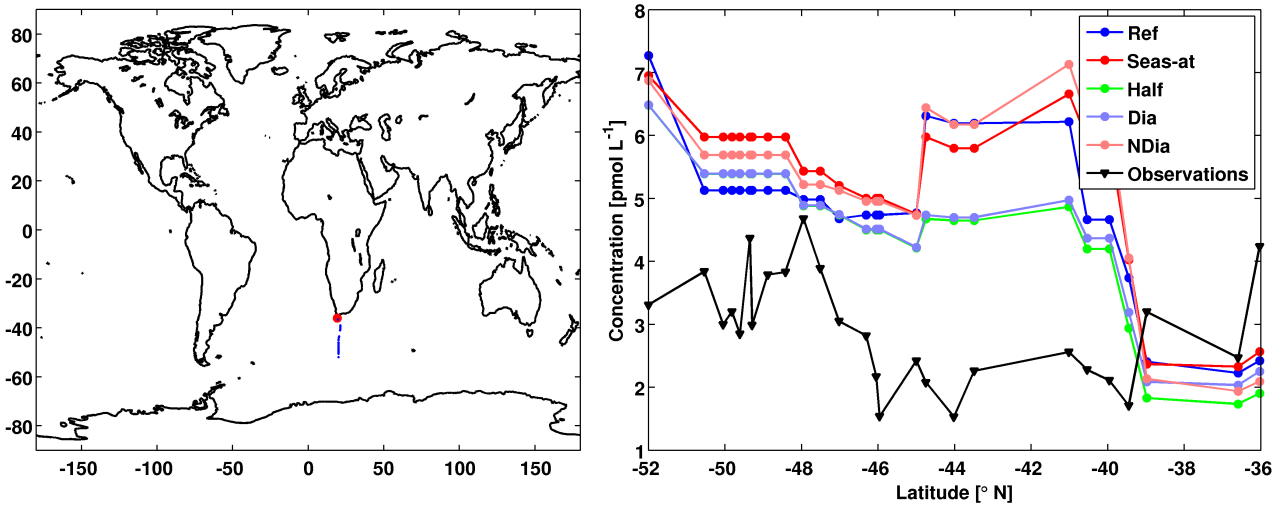

Figure S48 Observations are from the Polarstern cruise ANT XVIII/2 in October 2000 as listed in the SI of (Ziska et al., 2013).

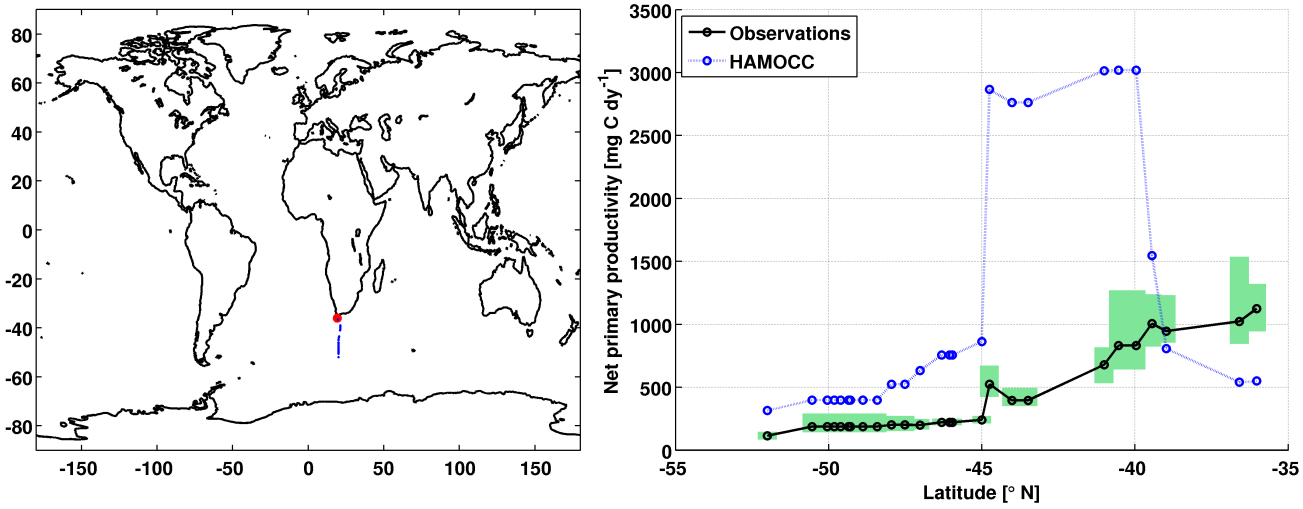

Figure S49 Simulated and observation-based net primary productivity [mg C m^{-2} dy^{-1}]. Green shades show mimimum and maximum range of the observation-based estimate, the black dashed line shows the median. The observation-based NPP product is based on data 1997-2009 from SeaWiFS Chl-*a*, PAR and AVHRR SST and derived using the VGPM model (Behrenfeld and Falkowski, 1997). The NPP producted was downloaded from http://wiki.icess.ucsb.edu/measures/NPP_Products (accessed June 2014).

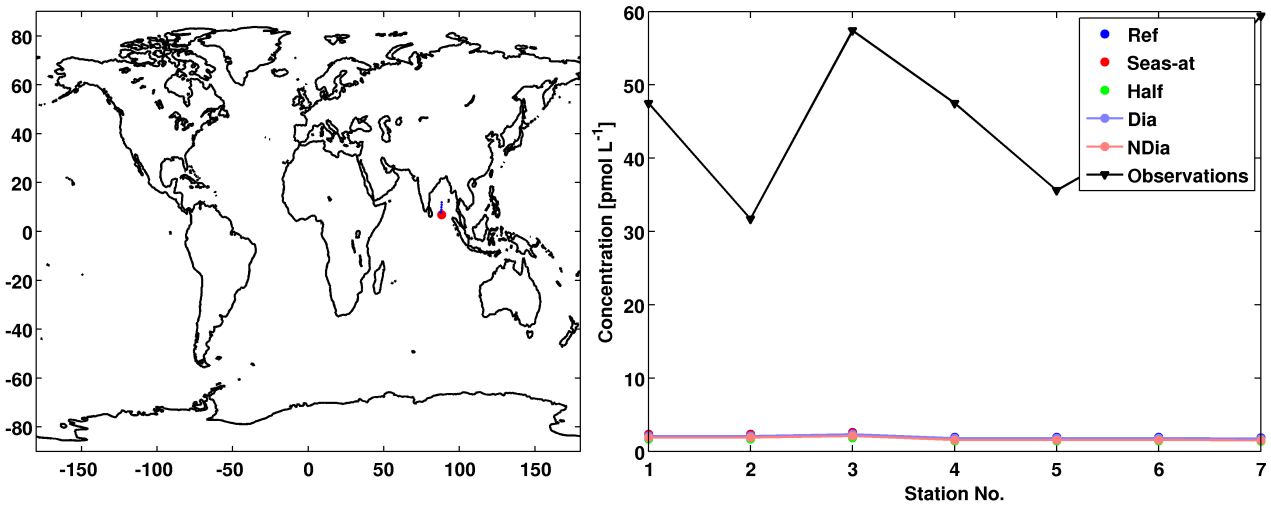

Figure S50 Observations are from the Shinyo-Maru cruise in the Bay of Bengal in Januar 1995 (Yamamoto et al., 2001) as listed in the SI of (Ziska et al., 2013).

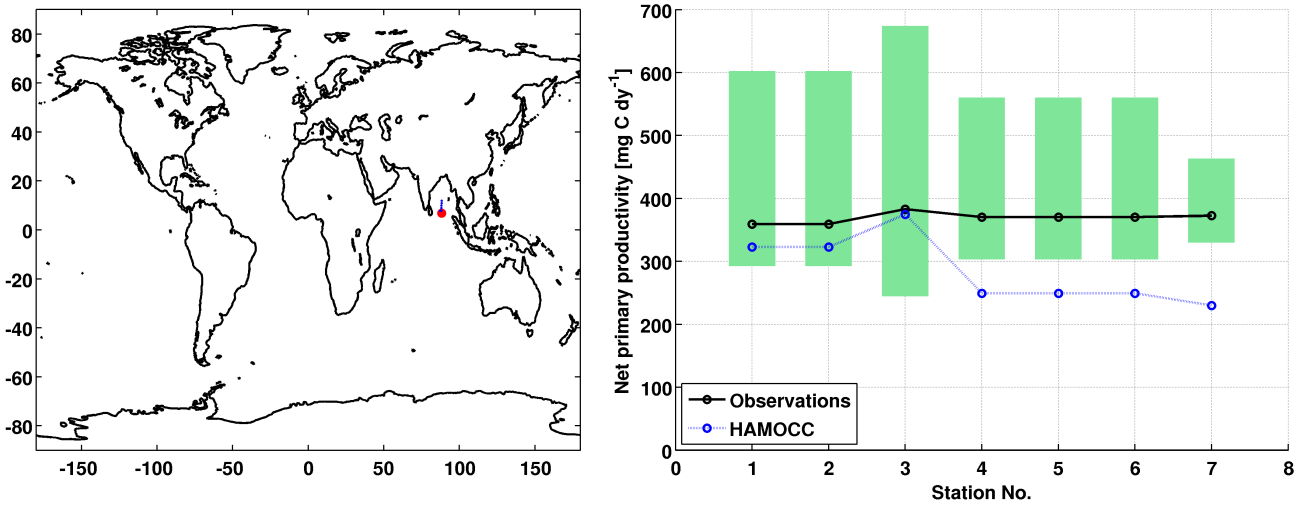

Figure S51 Simulated and observation-based net primary productivity [mg C m^{-2} dy^{-1}]. Green shades show mimimum and maximum range of the observation-based estimate, the black dashed line shows the median. The observation-based NPP product is based on data 1997-2009 from SeaWiFS Chl-*a*, PAR and AVHRR SST and derived using the VGPM model (Behrenfeld and Falkowski, 1997). The NPP producted was downloaded from http://wiki.icess.ucsb.edu/measures/NPP_Products (accessed June 2014).

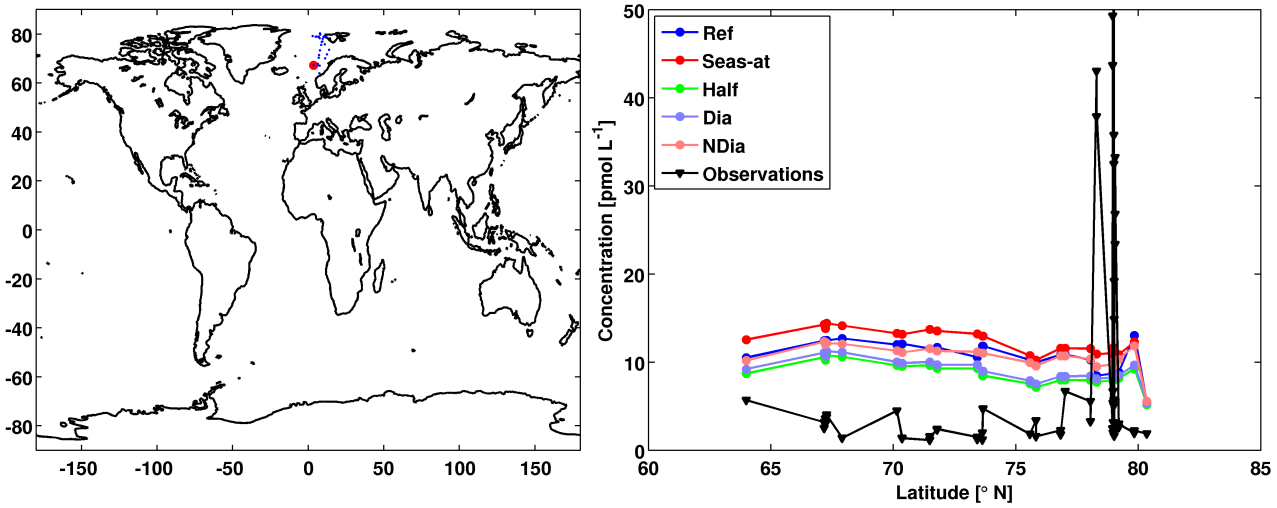

Figure S52 Observations are from the James Clark Ross cruise SAMS northen seas program (JR75) in June 2002 as listed in the SI of (Ziska et al., 2013).

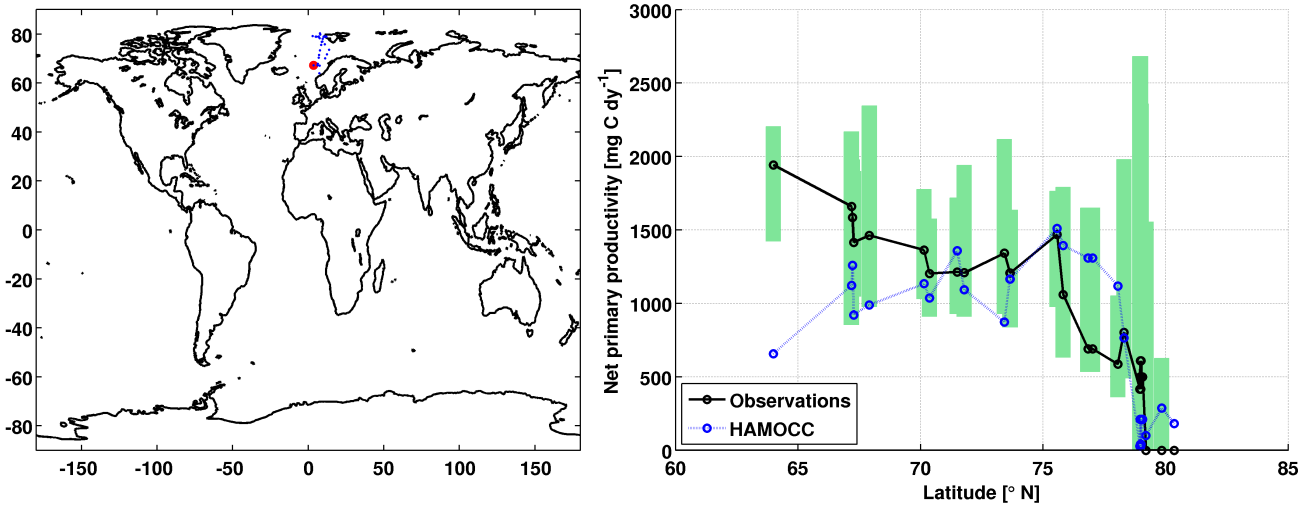

Figure S53 Simulated and observation-based net primary productivity [mg C m^{-2} dy^{-1}]. Green shades show mimimum and maximum range of the observation-based estimate, the black dashed line shows the median. The observation-based NPP product is based on data 1997-2009 from SeaWiFS Chl-*a*, PAR and AVHRR SST and derived using the VGPM model (Behrenfeld and Falkowski, 1997). The NPP producted was downloaded from http://wiki.icess.ucsb.edu/measures/NPP_Products (accessed June 2014).

References

Abrahamsson, K., Bertilsson, S., Chierici, S., Fransson, A., Froneman, P., Lorén, A., and Pakhomov, E.: Variations of biochemical parameters alonga transect in the Southern Ocean, with special emphasis on volatile halogenated organic compounds, Deep-Sea Res. II, 51, 2745–2756, 2004.

Baker, J., Reeves, C., Nightingale, P., Penkett, S., Gibb, S., and Hatton, A.: Biological production of methyl bromide in the coastal waters of the North Sea and open ocean of the northeast Atlantic, Marine Chemistry, 64, 267 – 285, doi:http://dx.doi.org/10.1016/S0304-4203(98)00077-2, 1999.

Behrenfeld, M. and Falkowski, P.: Photosynthetic rates derived from satellite-based chlorophyll concentration, Limnology and Oceanography, 42, 1–20, 1997.

Butler, J., King, D., Lobert, J., Montzka, S., Yvon-Lewis, S., Hall, B., Warwick, N., Mondell, D., Aydin, M., and Elkins, J.: Oceanic distributions and emissions of short-lived halocarbons, Glob. Biogeochem. Cyc., 21, 2007.

Chuck, A., Turner, S., and Liss, P.: Oceanic distributions and air-sea fluxes of biogenic halocarbons in the open ocean, Journal of Geophysical Research C: Oceans, 110, 1–12, 2005.

Jones, C., Hornsby, K., Sommariva, R., Dunk, R., Von Glasow, R., McFiggans, G., and Carpenter, L.: Quantifying the contribution of marine organic gases to atmospheric iodine, Geophysical Research Letters, 37, 2010.

Quack, B., Atlas, E., Petrick, G., Stroud, V., Schauffler, S., and Wallace, D.: Oceanic bromoform sources for the tropical atmosphere, Geophysical Research Letters, 31, 1–4, 2004.

Quack, B., Atlas, E., Petrick, G., and Wallace, D.: Bromoform and dibromomethane above the Mauritanian upwelling: Atmospheric distributions and oceanic emissions, Journal of Geophysical Research D: Atmospheres, 112, 2007.

Schall, C., Heumann, K., and Kirst, G.: Biogenic volatile organoiodine and organobromine hydrocarbons in the Atlantic Ocean from 42 N to 72 S, Fresenius' Journal of Analytical Chemistry, 359, 298–305, 1997.

Yamamoto, H., Yokouchi, Y., Otsuki, A., and Itoh, H.: Depth profiles of volatile halogenated hydrocarbons in seawater in the Bay of Bengal, Chemosphere, 45, 371–377, 2001.

Ziska, F., Quack, B., Abrahamsson, K., Archer, S. D., Atlas, E., Bell, T., Butler, J. H., Carpenter, L. J., Jones, C. E., Harris, N. R. P., Hepach, H., Heumann, K. G., Hughes, C., Kuss, J., Krüger, K., Liss, P., Moore, R. M., Orlikowska, A., Raimund, S., Reeves, C. E., Reifenhäuser, W., Robinson, A. D., Schall, C., Tanhua, T., Tegtmeier, S., Turner, S., Wang, L., Wallace, D., Williams, J., Yamamoto, H., Yvon-Lewis, S., and Yokouchi, Y.: Global sea-to-air flux climatology for bromoform, dibromomethane and methyl iodide, Atmospheric Chemistry and Physics, 13, 8915–8934, doi:10.5194/acp-13-8915-2013, 2013.